New Jersey Institute of Technology
Digital Commons @ NJIT

Theses | Electronic Theses and Dissertations

8-30-1991

A microengineered beam diaphragm structure for the high performance pressure sensor

Alkesh Shah
New Jersey Institute of Technology

Follow this and additional works at: https://digitalcommons.njit.edu/theses

 Part of the Electrical and Electronics Commons

Recommended Citation

Shah, Alkesh, "A microengineered beam diaphragm structure for the high performance pressure sensor" (1991). *Theses*. 2609.
https://digitalcommons.njit.edu/theses/2609

This Thesis is brought to you for free and open access by the Electronic Theses and Dissertations at Digital Commons @ NJIT. It has been accepted for inclusion in Theses by an authorized administrator of Digital Commons @ NJIT. For more information, please contact digitalcommons@njit.edu.

Copyright Warning & Restrictions

The copyright law of the United States (Title 17, United States Code) governs the making of photocopies or other reproductions of copyrighted material.

Under certain conditions specified in the law, libraries and archives are authorized to furnish a photocopy or other reproduction. One of these specified conditions is that the photocopy or reproduction is not to be "used for any purpose other than private study, scholarship, or research." If a, user makes a request for, or later uses, a photocopy or reproduction for purposes in excess of "fair use" that user may be liable for copyright infringement,

This institution reserves the right to refuse to accept a copying order if, in its judgment, fulfillment of the order would involve violation of copyright law.

Please Note: The author retains the copyright while the New Jersey Institute of Technology reserves the right to distribute this thesis or dissertation

Printing note: If you do not wish to print this page, then select "Pages from: first page # to: last page #" on the print dialog screen

NJIT New Jersey's Science & Technology University

The Van Houten library has removed some of the personal information and all signatures from the approval page and biographical sketches of theses and dissertations in order to protect the identity of NJIT graduates and faculty.

ABSTRACT

Title of Thesis: A Microengineered Beam Diaphragm Structure for the High Performance Pressure Sensor

Alkesh Shah, Master of Science, Electrical Engineering Department, 1991

Thesis directed by: Dr. D. Misra, Assistant Professor

The thesis details the design for a novel microengineered beam diaphragm structure for piezoresistive pressure sensor applications. The beam diaphragm structure is used as a pressure sensing device, within a wheatstone bridge circuit. The single crystal silicon with [100] orientation is used for the beam diaphragm structure.

It has the advantages of high sensitivity(2.56 v/v/mm of Hg), good linearity(3Kpa to 1.4 Mpa) and overpressure protection with the help of the bosses. It's protection range is about 400 times the standard pressure range. The beam diaphragm structure has two rectangular bosses which are formed by anisotropic etching. Two pairs of diffused piezoresistive elements are located on the top surface of the diaphragm such that higher sensitivity can be obtained. Finite Element Method is used to analyse the load deflection behavior of the beam diaphragm structure. Results of the Finite Element Method using ANSYS program are presented. Analytical results are compared with FEM results and verified. The micromachining process for the fabrication is also described.

A Microengineered Beam Diaphragm Structure for the High Performance Pressure Sensor

by

Alkesh Shah

Thesis submitted to the Faculty of the Graduate School of
the New Jersey Institute of Technology
in partial fulfillment of the requirements for the degree of
Master of Science in Electrical Engineering

October 1991

APPROVAL SHEET

Title of Thesis: A Microengineered Beam Diaphragm Structure for the High Performance Pressure Sensor

Name of Candidate: ALKESH SHAH
Master of Science in Electrical Engineering, 1991

Thesis and Abstract Approved: _____ _____

Dr. D. Misra — Date
Assistant Professor
EE Department

_____ _____

Dr. K. Sohn — Date
Professor
EE Department

_____ _____

Dr. N. M. Ravindra — Date
Associate Professor
Physics Department

VITA

Name: ALKESH SHAH

Address:

Degree and date to be conferred: MSEE, 1991

Date of birth:

Place of birth

Collegiate institutions attended	Dates	Degree	Date of Degree
M. S. University, Baroda, India	1984-1988	BSEE	Dec. 1988
New Jersey Institute of Technology	1989-1991	MSEE	Oct. 1991

Major: Electrical Engineering

To My Parents

Acknowledgement

First of all, I would like to thank my thesis advisor, Dr. D. Misra. He not only gave me technical advice on my work, but also provided me with a comfortable working atmosphere. His unfailing encouragement gave me the strength to continue my work even when the obstacles seemed insurmountable.

I also acknowledge the financial support provided by Dr. D. Misra at New Jersey Institute of Technology.

Special thanks to my friends Milind Patel, Paresh Patel and Mehul Patel for their encouragement.

I also wish to thank my parents and my family for their generous and caring support during my entire study.

Contents

1 Introduction 1
- 1.1 An Overview . . . 1

2 Diphragm Structures 4
- 2.1 Introduction . . . 4
- 2.2 Circular Diaphragms . . . 5
- 2.3 Square Diaphragms . . . 8
- 2.4 Beam Diaphragm Structure . . . 9

3 Modeling of Beam Diaphragm Structure 12
- 3.1 Introduction . . . 12
- 3.2 Beam's Equation . . . 13
- 3.3 Simply Supported Square Plates . . . 14
- 3.4 Beam Diaphragm Structure . . . 17
- 3.5 Finite Element Method For Film Deflection . . . 17
  - 3.5.1 Basic Concept of Finite Element Method . . . 18
  - 3.5.2 Type of Elements . . . 19
- 3.6 ANSYS Program . . . 20
  - 3.6.1 Preprocessing . . . 22
  - 3.6.2 Solution Phase . . . 23
  - 3.6.3 Post Processing . . . 23

4 Simulation Results 24
- 4.1 Results of ANSYS Simulations . . . 24
- 4.2 Load Deflection Behavior . . . 26

5 Design of Piezoresistive Pressure Sensor 38
- 5.1 Introduction . . . 38
- 5.2 Piezoresistance Coefficient . . . 39
- 5.3 Piezoresistive Beam Diaphragm Structure . . . 41
- 5.4 Size of Resistors . . . 42
- 5.5 Sensitivity . . . 44
- 5.6 Micromachining Process . . . 47

5.6.1 Bulk Micromachining 47
5.6.2 Surface Micromachining 49
5.6.3 Proposed Micromachining Process 49

6 Conclusion **52**

Appendix **54**

Bibliography 80

List of Figures

2.1 Basic structure of a piezoresistive pressure sensor. [Ref. 4] 5
2.2 Circular diaphragm 6
2.3 Single island circular diaphragm structure. 6
2.4 Twin island diaphragm structure. 7
2.5 The layout of the rectangular diaphragm. 8
2.6 Typical geometries for low pressure sensors. [Ref. 10] 9
2.7 Beam diaphragm structure 10

3.1 Cross section of a suspended film undergoing a center deflection d at an applied pressure P. 14
3.2 The displacement and forces in the deflection of a square film (a) the geometry of the film; (b) the displacement u and w; (c) the force balance in film deflection. 15
3.3 STIF 82 2-D 8-node element. (a) Geometry of the element (b) Element stress directions 21
3.4 Modes of operation 22

4.1 Finite Element Modeling of the beam diaphragm structure. Different color indicates the elements. 27
4.2 Stress distribution in beam diaphragm structure under the applied pressure. The different color indicates the average value of the stresses. 28
4.3 Magnified view of the tensile stresses. 29
4.4 Magnified view of the compressive stresses. 30
4.5 Deformation of the beam diaphragm structure after the application of load. 31
4.6 Stress distribution along the number of elements on the beam diaphragm structure. 32
4.7 Over pressure protection for the beam diaphragm structure. 33
4.8 Pressure versus maximum/minimum stress curves. 34
4.9 FEM results: pressure versus deflection curve. 35
4.10 FEM results: P/d versus d^2 curve. 36

5.1 Piezoresistance factor P(N,T) as a function of impurity concentration and temperature for n-Si. [Ref. 24] 40

5.2 Piezoresistance factor P(N,T) as a function of impurity concentration and temperature for p-Si. [Ref. 24] 41
5.3 Resistivity change with impurity concentration. [Ref.21] 43
5.4 Variation of sensitivity with different location of resistors. 46
5.5 Proposed Micromachining Process 51

List of Tables

5.1 Approximate piezoresistance coefficients at room temperature [Ref. 19] 40
5.2 Resistivity change with impurity concentration 44
5.3 Values of sensitivity with different location of the resistors. 45

Chapter 1

Introduction

1.1 An Overview

The rapid progress in VLSI semiconductor technology has increased the capabilities of realizing solid state microsensors. Mechanical sensors, pressure sensors, temperature sensors and magnetic sensors are recently being used in Research. There is now growing demand for small, reliable and low cost solid state sensors capable of interfacing with natural events. Pressure measurements are essential in many areas, including biomedical research and clinical care, as well as automobiles and industrial process control. Therefore the pressure transducer is one of the most widely used physical transducers. A variety of commercial pressure transducers are available to meet the present needs, but continuous efforts have been made to seek new miniature, long term stable and sensitive devices for specialized applications. Three basic

types of silicon pressure transducers have been reported:piezojunction[1], piezoresistive[2], and capacitive pressure transducers[3]. Of these three basic types of silicon transducers, the piezoresistive device is presently the most widely used pressure transducer because of its high performance and ease of design and fabrication.

In many applications, it is highly desirable to obtain both high sensitivity to low values of applied pressure and tolerance to very high pressure without failures. Although the strength of silicon is very high, the thin diaphragm of a conventional silicon pressure sensor will typically fail at pressures in the range of 10-30 times rated full scale pressure. Very high overpressure tolerances are impossible using conventional sensor structures in which the diaphragm is suspended at its edges, such that its deflection increases unimpeded as pressure increases.

In order to solve this difficulty a novel micromachined beam diaphragm structure for the pressure sensor application is developed. The beam diaphragm structure represents a new class of structure which has beams connected with diaphragm for utilizing the maximum stress concentration area. Overpressure protection is obtained for this type of sensor, since the diaphragm can only deflect by a distance set by the bosses before reaching and being stopped by the silicon bottom. The sensor is a piezoresistive bridge diffused on a (100) oriented wafer. By proper selection the diaphragm geometry, the bridge output is linear with pressure and more reproducible than previous designs.

The thesis is organised in five parts. The first part chapter2 describes different diaphragm structures which are used for the pressure sensor applications. Their advantages and disadvantages are also discussed. Chapter3 discusses the analytical and finite element model for the film deflection. The ANSYS program for simulation is also explained. Chapter4 contains the results obtained from the simulation. The most of the results are explained by figures. The design of the piezoresistive pressure

sensor is described in the chapter5. It contains the theory of piezoresistors and calculation of diaphragm parameters. Chapter 6 details the conclusion, various applications and also suggests some helpful improvements which will further enhance the viability of this work. The ANSYS input-output file is given in Appendix.

Chapter 2

Diaphragm Structures

2.1 Introduction

The basic structure of a solid state pressure sensor is shown in fig. 2.1. The main structure is a silicon diaphragm in to which silicon resistor tracks are introduced by ion implantation. Pressure exerted on the diaphragm causing it to expand results in change in resistance on the principle of piezoresistive effect. Most silicon piezoresistive pressure sensor comprise a bridge of four piezoresistors or a Hall-type strain gauge on a silicon diaphragm. The diaphragm is essentially a mechanical structure that converts the applied pressure to either tensile or compressive stress. It has become more and more clear that this conversion plays a very important role in deciding the performance of pressure sensor. The configurations of the diaphragms so far being used are a circular diaphragm , square diaphragm and a rectangular

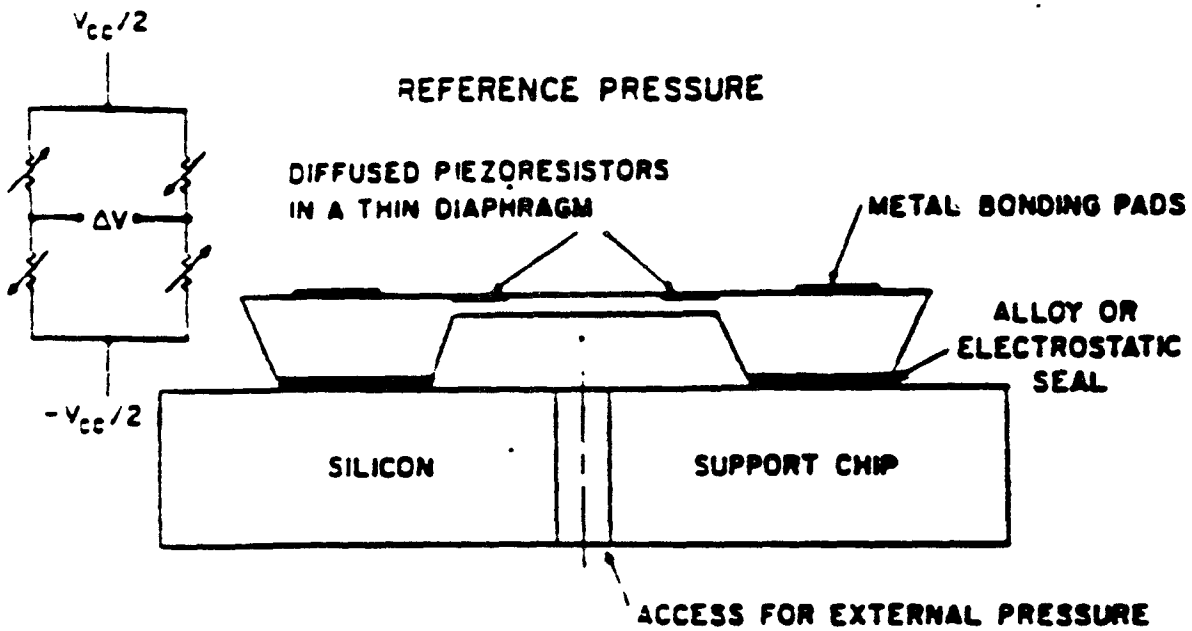

Figure 2.1: Basic structure of a piezoresistive pressure sensor. [Ref. 4]

diaphragm.

2.2 Circular Diaphragms

In 1960s, circular flat diaphragms[5] processed by mechanical drilling and isotropic chemical etching were commonly used. The circular diaphragm is mainly used in biomedical applications on the tip of the catheter. Although they have wide applications, the circular diaphragm has poor controllability and accuracy. In order to enhance the sensitivity of these pressure sensor, the silicon diaphragm has to be made very thin. Because of the large deflection of the thin diaphragm due to the applied pressure, the nonlinearity is incresed by few percent. The fig. 2.2 shows the simple circular diaphragm which generally used for the biomedical applications.

For a flat diaphragm with a lateral dimension a and thickness h, it is well known that [6] the stress(T) is proportional to $P(\frac{a}{h})^2$, where P is the applied pressure. It seems that a very sensitive pressure sensor can be produced by making $\frac{a}{h}$ large enough. However, as the nonlinearity of the pressure to stress conversion is pro-

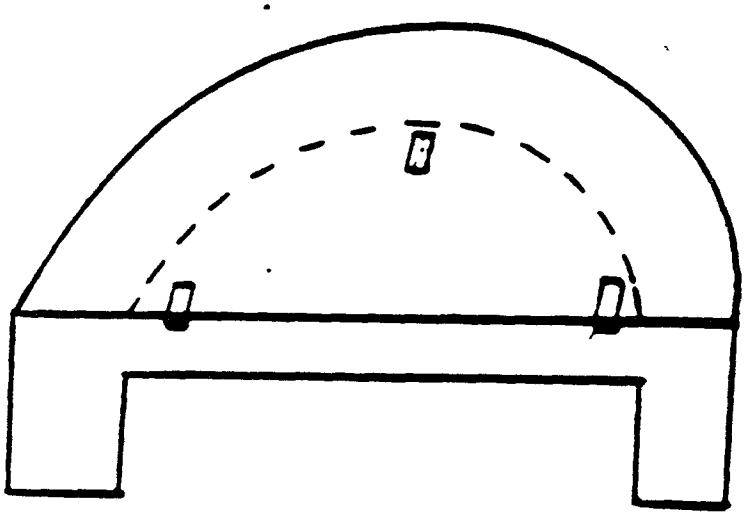

Figure 2.2: Circular diaphragm

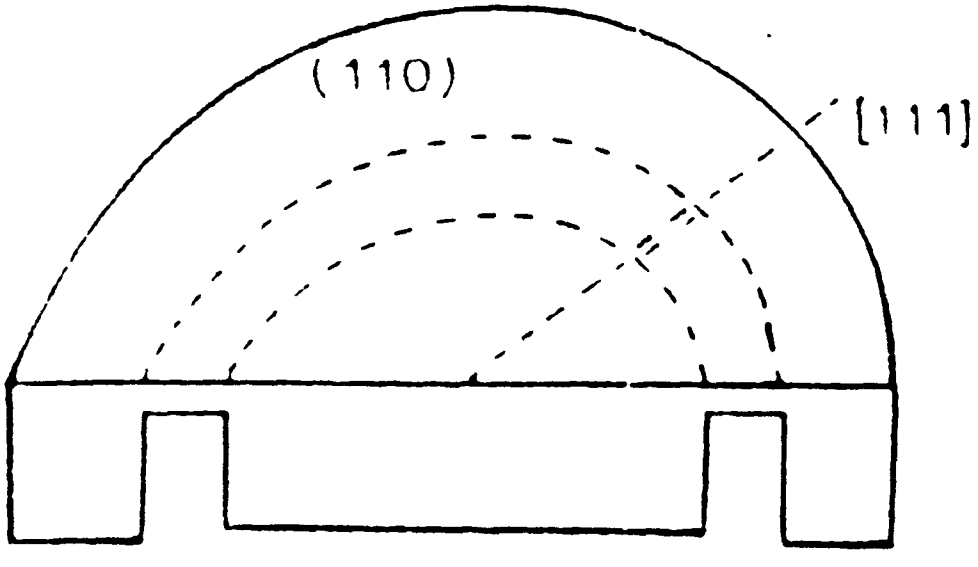

Figure 2.3: Single island circular diaphragm structure.

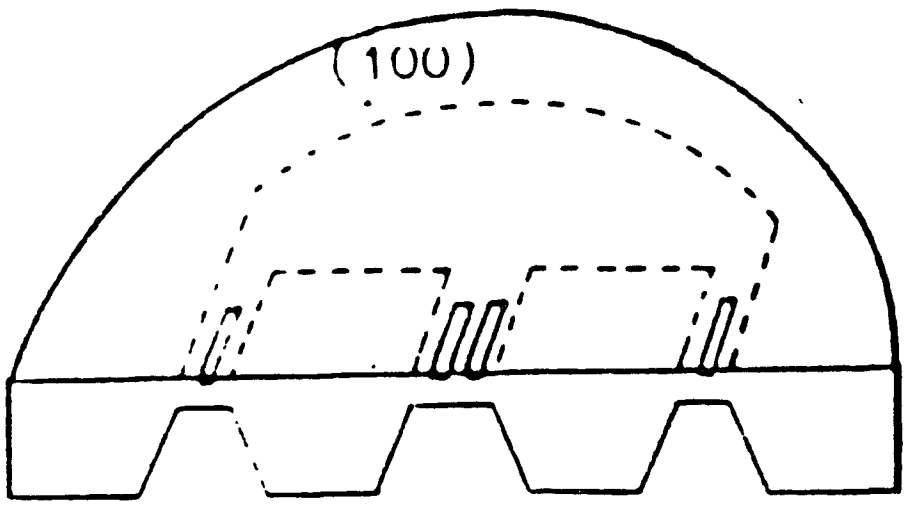

Figure 2.4: Twin island diaphragm structure.

portional to $P(\frac{a}{h})^4$ [7], severe nonlinearity might make a high sensitivity device of little practical when $\frac{a}{h}$ is beyond a certain limit. Making a pressure transducer with both high sensitivity and good linearity was of main goals of many innovations made in 1980s. Shimazoe et al. [8] proposed a circular diaphragm with a concentric island on the back of the diaphragm, as shown in Fig. 2.3. By this structure, they developed an accurate pressure transducers for the low pressure range.

In this structure, the thin diaphragm is a ring on which stress changes rapidly from a positive maximum on one side to a negative maximum on other side, zero near middle. To accommodate two pairs of radial resistors on the ring area, the tolerance for double sided alignment is tight and the chip can hardly be miniaturized. The Endevco Co.[9] used a structure combining a diaphragm with two islands, as shown in fig. 2.4. By this design, high sensitivity and good linearity could be achieved simultaneously because of stress concentration at the narrow diaphragm areas and nonlinearity compensation among the resistors all subjected to lateral stresses. However this process requires very tight process control.

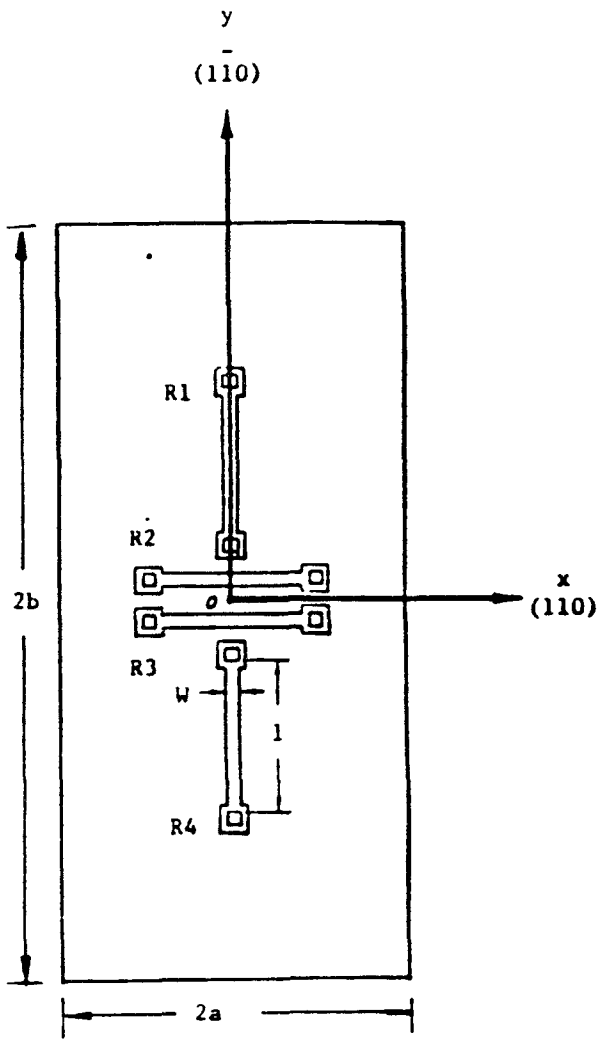

Figure 2.5: The layout of the rectangular diaphragm.

2.3 Square Diaphragms

In 1970s square and rectangular flat diaphragms processed by anisotropic chemical etching prevailed. Compared to square diaphragm, it seems the circular diaphragm is inferior in aspects such as sensitivity, symmetry and simplicity of processing. Both the square diaphragm and rectangular diaphragm have some advantages and disadvantages. Theoratically higher sensitivity can be achieved by using the square diaphragms. However, the pressure sensitivity drops dramatically when position of the resistors shifts from the edge, due to alignment error or back etch, or when the

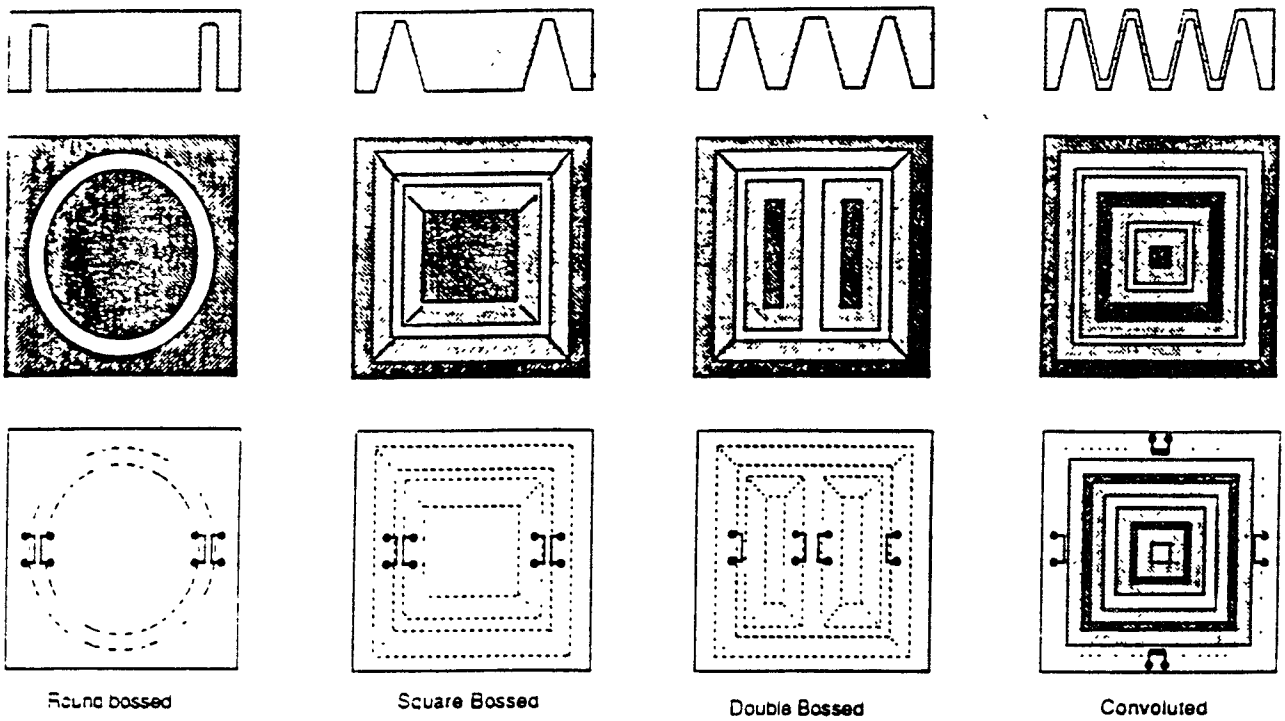

Figure 2.6: Typical geometries for low pressure sensors. [Ref. 10]

the resistors extend towards the center area due to an increased width for better symmetry. Fig. 2.5 shows the layout of rectangular diaphragm for the pressure sensors. For the low pressure applications and in order to achieve acceptable linearity, a number of geometries have been employed by several investigators. These includes square bossed, double bossed square and convoluted structure which are shown in fig. 2.6. The die size of this devices are approximately3 $\times$ 2.5mm. Typical diaphragm thicknesses vary from 2 to 12um for 1psi ranges and below. To obtain the required precision, one of the several available etchstop techniques must be employed.

2.4 Beam Diaphragm Structure

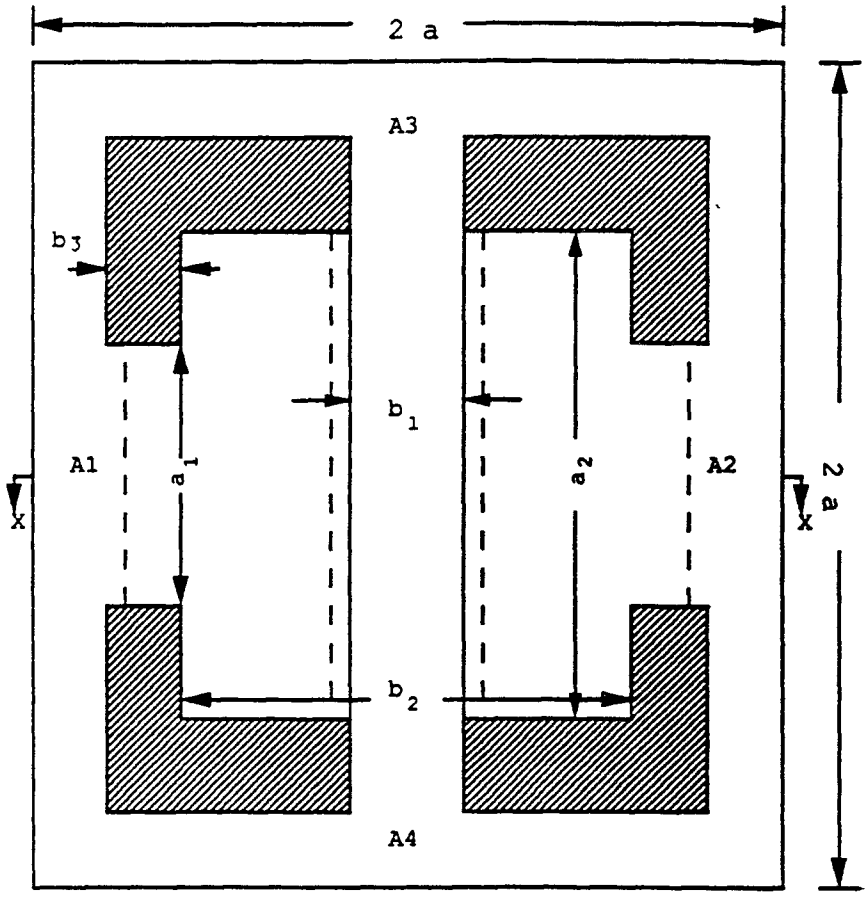

(a) TOP VIEW

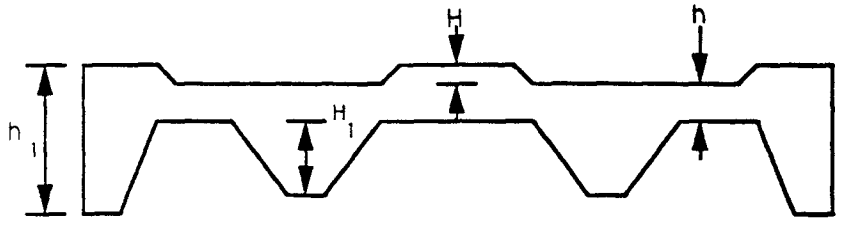

(B) SECTION XX

Figure 2.7: Beam diaphragm structure

To achieve excellent performances on sensitivity and linearity but without the drawbacks of circular and square diaphragms, novel beam diaphragm structures[11] are proposed. It has advantages in all aspects over the existing structures, while having the advantages of high sensitivity and good linearity as double island diaphragm structures. The additional advantages of the new structure designed as a part of this work are overpressure protection and ease of double sided alignment. Furthermore selective chemical etching can be adapted to process thin diaphragms and back islands are provided for overpressure protection.

Fig. 2.7 shows the geometry of the new beam diaphragm structure. It has four beams, one on each side of the diaphragm. Beams are etched for the purpose of the good linearity and high sensitivity. Fig. 2.7 shows the topview of the geometry as well as the section XX. Regions A3 and A4 has a support from the structures which are adjacent to them. The square diaphragms with beams on the each side can be processed by micromachining technique [10]. A deep back anisotropic etching can be used to form the bosses. A variety of etchants like KOH, EDP and electrochemical can be employed to achieve the geometry. Diaphragm thickness can be varied from 4um to 12um. When the pressure is applied to the diaphragm A1 and A2 will experience a tensile stress where as center part of the diaphragm will have compressive stress. The stress is first concentrated from the diaphragm to the beam due to thickness difference. The stress is further concentrated at the narrow regions of the beam due to difference in width. The typical parameters for the beam diaphragm structure are H=5μm, H_1=63μm, h=10μm, h_1 = 100μm, a=300μm $a_1 = 300\mu m$, $a_2 = 450\mu m$, $b_1 = 35\mu m$, $b_2 = 382\mu m$, $b_3 = 15\mu m$. Following chapters will give the detail design of the beam diaphragm structure.

Chapter 3

Modeling of Beam Diaphragm Structure

3.1 Introduction

In this chapter the analytical and Finite Element Method(FEM) model for the load deflection behavior of the suspended film is developed and applied to the beam diaphragm structure. The purpose for this analysis is to find the functional form of the relationship between pressure and deflection. That is, the analytical solution provides formulas for the relationship between pressure and deflection. FEM provides more accurate deformed shapes.

Over the past two or three years, numerical modeling of the sensors and microstructures has gradually been developed as an integral part of the microsensor design process. Recent achievements [12] in successful finite element modeling(FEM)

of fabricated devices could play a major role in further adoption and implementation of numerical modeling through the sensor and micromachining field.

In section 3.2 Beam's equation for the deflection of the thin film is explained. In section 3.3 the models for the square films are derived. In this thin film model membrane like behavior is assumed. That is, the bending effect at the edge of the deformed film is neglected. However as the films get thicker, the bending effect has to be considered. In section 3.4 analytical model for the beam diaphragm structure is developed. The results of the models shows the relationship between pressure and deflection for the square films. Section 3.5 describes finite element modeling for the film deflection. It contains the information regarding the basic concepts and type of element used for the simulations. Section 3.6 discusses the ANSYS program used for the FEM.

3.2 Beam's Equation

A mechanical model for deflection of thin film has been developed by Beams [13]. A typical cross section of a deflected film under lateral pressure is shown in Fig. 3.1. In Beam's equation, the relationship between pressure P and stress T is assumed first that

$$P = \frac{4hTd}{a^2} \tag{3.1}$$

where T is the stress along the plane of film, d is deflection, a is the distance from the center to the edge of film, h is a film thickness, and P is the pressure. The stress T is a sum of the stretching stress and the residual stress.

$$T = \frac{E}{1-\nu}\varepsilon + \sigma_0 \tag{3.2}$$

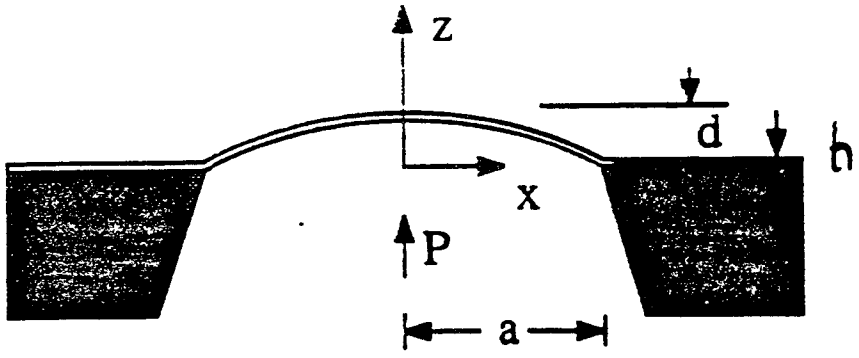

Figure 3.1: Cross section of a suspended film undergoing a center deflection d at an applied pressure P.

where ε is the average strain of the film, E is young's modulus, ν is inplane poisson ratio, and σ_0 is residual stress. By substituting Eq. 3.2 into 3.1 and solving,

$$\frac{Pa^2}{hd} = (\frac{4E}{1-\nu})\,\varepsilon + 4\sigma_0 \tag{3.3}$$

The average strain is given by a relation,

$$\varepsilon = \frac{2d^2}{3a^2} \tag{3.4}$$

By substituting Eq. 3.4 into Eq. 3.3, the final form [14] of Beam's equation is written

$$\frac{Pa^2}{hd} = C_2\frac{1}{a^2}(\frac{4E}{1-\nu})\,d^2 + C_1\sigma_0 \tag{3.5}$$

where $C_2 = 8/3$ and $C_1 = 4$.

3.3 Simply Supported Square Plates

A mechanical model for deflection of the square films is developed. A typical top view of a square film is shown in Fig. 3.2(a). A deflected film under lateral pressure

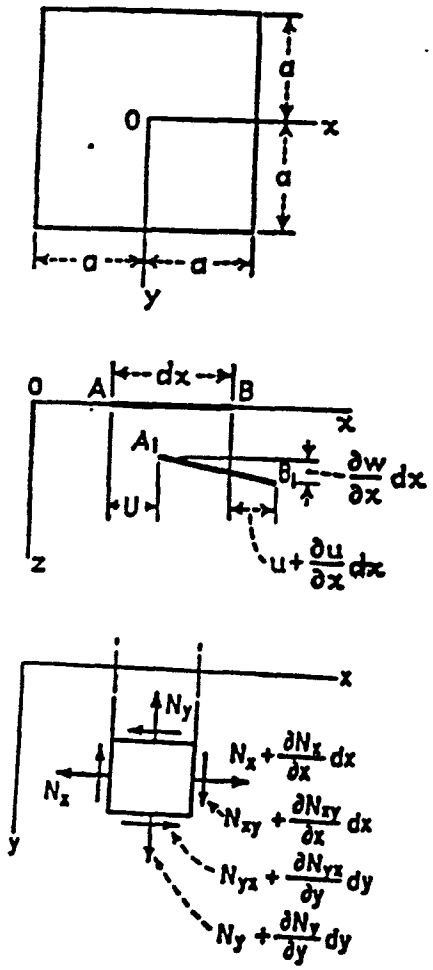

Figure 3.2: The displacement and forces in the deflection of a square film (a) the geometry of the film; (b) the displacement u and w; (c) the force balance in film deflection.

under lateral pressure is shown in Fig. 3.2(b). In this section, an energy minimization approach for the film deflection is used. Several assumption are made in this mechanical analysis of the film deflection. First it is assumed that the thickness of the film is very small compared to the size of the diaphragms. The bending energy of the deflected membrane is neglected under this assumption. Third, plane stress is assumed. That is, stress is entirely in the plane of the film as the film is deflected. Forth, the residual stress of the film due to the manner of fabrication is a constant and is biaxially distributed in the plane of the film. Residual stress is also assumed

uniform throughout the thickness of the film [15]. Fifth, the film is assumed in the linear elastic regime as it is deflected. The functions of the displacements of the deflected membrane are assumed as[16]:

$$w = d\cos(\frac{\pi x}{2a})\cos(\frac{\pi y}{2a}) \tag{3.6}$$

$$u = c\cos(\frac{\pi x}{a})\cos(\frac{\pi y}{2a}) \tag{3.7}$$

$$v = c\sin(\frac{\pi y}{a})\cos(\frac{\pi x}{2a}) \tag{3.8}$$

Where u, v and w are the displacements along the X, Y and Z axes respectively, c and d are the constants to be determined. 2a is the size of the diaphragm. Here w fits the boundary conditions that the zero at the edge and maximum at the center. Also the displacement u and v fit the boundary conditions that zero at both the center and the edge of the membrane.

Using the energy minimization method, based on Eqs. 3.6-3.8, pressure deflection relation can be derived. The details of the calculation is shown in reference [16] and only the result is presented here. For the square membrane of the side length 2a, the load-deflection relation is:

$$(\frac{Pa^2}{hd}) \;=\; C_2\,(\nu)\,(\frac{E}{1-\nu})\,(\frac{1}{a^2})\,d^2 \;+\; C_1\sigma_0 \tag{3.9}$$

where

$$C_2(\nu) \;=\; \frac{\pi^6}{32(1+\nu)}[(\frac{5}{64}) \;-\; \frac{(5-3\nu)^2}{[64(1+\nu) \;+\; 9\pi^2(9-\nu)]}] \tag{3.10}$$

$$C_1 = \pi^4/32 \tag{3.11}$$

P is a applied pressure, E is the young's modulus, $\frac{E}{1-\nu}$ is the biaxial modulus, σ_0 is the residual stress, ν is the poisson ratio , h is thickness, and d is the deflection at the center of the diaphragm.

3.4 Beam Diaphragm Structure

For the beam diaphragm structure, the thickness of the diaphragm is not constant between the two edges as shown in Fig. 2.7. At the center of the beam diaphragm structure considering H and h both, the load deflection relation is:

$$\frac{Pa^2}{(h+H)d} = C_2(\nu)\,(\frac{E}{1-\nu})\,(\frac{1}{a^2})\,d^2 + C_1\sigma_0 \tag{3.12}$$

For single crystal silicon, ν= 0.42 [18]

Using this value, the values of the constants are:

$$C_1 = \pi^4/32 = 3.044 \tag{3.13}$$

$$C_2(\nu) = \frac{\pi^6}{32(1+\nu)}[(\frac{5}{64}) - \frac{(5-3\nu)^2}{[64(1+\nu) + 9\pi^2(9-\nu)]}] = 1.306 \tag{3.14}$$

Comparing this equation with Beam's equation(Eq. 3.5), several similarity are worth mentioning. First of all C_2 is not a function of poisson's ratio in Beam's equation, while it is linearly Poisson ratio dependant in Eq. 3.12. Second both equations shows that the general form for the relationship between pressure and deflection which has two terms: biaxial modulus term($\frac{E}{1-\nu}$) and residual stress term(σ_0).

3.5 Finite Element Method For Film Deflection

In the design of silicon sensors and microstructures, a multitude of thin films, such as oxide and metal, are grown and deposited at different process steps to achieve certain mechanical and physical geometries and functions. Due to certain mechanical and physical properties of these films the device usually experiences various thermal and mechanical loads resulting in displacements and stresses which are often not easy to predict by analytical approaches. This becomes more critical as the device become smaller and more mechanically complex, while related sub-components(

beams, diaphragms, etc.) become thinner. Accurate prediction of the behavior of these type of the structures could benefit process design, device performance and demonstrate its limits imposed by undesirable environmental factors. Finite element modeling (FEM) has been a standard numerical modeling technique extensively utilized in structural engineering discipline for structure and component design. The application of this technique is gaining popularity and is becoming a standard design process in sensor industry.

The finite element method (FEM) is introduced here for the simulation of the load deflection behavior of the beam diaphragm structure. This simulated load deflection relationship was used for calculating the geometry and Poisson ratio dependent constants in the mathematical model. It is believed that the constants calculated using FEM are more accurate than using analytic solution due to more accurate deflected shapes predicted by FEM simulations.

3.5.1 Basic Concept of Finite Element Method

The finite element method(FEM) is generally applicable for numerical solutions. Problems of continuum mechanics, electric fields, heat transfer, and fluid flow have been solved using FEM [17]. In this study, FEM is used solely for mechanical analysis of the film deflection. The FEM used in this study is the commercially available ANSYS program (Swanson Analysis Systems, Inc.) which was run on SUN 3/60 workstation. The basic concepts of FEM are summerised and only the most general situation is described here. To solve a general problem of solid mechanics using FEM, several steps are followed:

- Discretize the body of solid.
- Select an interpretation model for elements.
- Calculate the element stiffness matrices and overall equilibrium equations.

- Calculate stresses.

In the first step, the actual body of solid(the film) is represented as a group of subdivisions called finite elements. These elements are considered to be interconnected at the specified joints called nodes or nodal points. The nodes are usually distributed on element boundaries and inside the elements. The nodes on the boundaries are shared with adjacent elements. The choice of type, number, size, and arrangement of the elements depends on the characteristics of the problem.

Next, it is assumed that the variation of the field variable(e. g. displacement, stress, etc.) inside a finite element can be approximated by a simple polynomial function(called interpolation model). For example, if the displacement is assumed, the model is called the assumed displacement model. In the third step, using the assumed displacement model and equilibrium equations, the element stiffness matrices and load vectors are assembled to form the overall equilibrium equations for the entire body.

Fourth, the overall equilibrium equations for the whole body are then incorporated into boundary conditions. At this point, a set of simultaneous equations(in matrix form) are generated. By solving these equations, the nodal values of the field is known, other field variables (such as stress, strain, etc.) throught the whole group of elements can then be calculated.

3.5.2 Type of Elements

In this study, deflections of thin films by lateral pressure was simulated by FEM. The type of element used for simulation of beam diaphragm structure is STIF 82.

It is a 2D 8-node isoparametric solid element. The 8-node elements have the

displacement shapes and are well suited to model curved boundaries. The 8-node element is defined by eight nodal points having two degrees of freedom at each node: translations in the nodal X and Y directions. The element may be used as a biaxial plane element or as an axiammetric ring element. The element has plasticity, creep, swelling and stress stiffening capabilities.

The geometry, nodal point locations, face numbers, loading and coordinate system for this element are shown in Fig.3.3(a). The element coordinate system is parallel to global cartesian coordinate system. Midside nodes may be removed(with zero node number) to form a pattern compatible with other element types. The geometric locations of midside nodes automatically calculated, if not supplied.

The triangular shaped element may be formed by defining the same node number for nodes K, L and O. Besides node, the element input data includes a thickness and material properties. The element stress directions are shown in Fig. 3.3(b). The directions are parallel to the global cartesian coordinate system. Surface stresses are defined parallel and perpendicular to the IJ face (and KL face) and along the Z axis for a plane analysis or in the loop direction for an axisymmetric analysis.

3.6 ANSYS Program

The ANSYS program is a self contained general purpose finite element program developed and maintained by Swanson Analysis systems, Inc. This program is designed to be user oriented and can be applied to wide variety of engineering problem. The program has numerous capabilities and options. In addition, the program flexibility allows various methods of arriving at the same solution. The program contains many routines, all inter related and all for the main purpose of achieving a solution to an engineering problem by finite element method. An engineering problem is usually solved in three phases. (1) preprocessing (2) solution

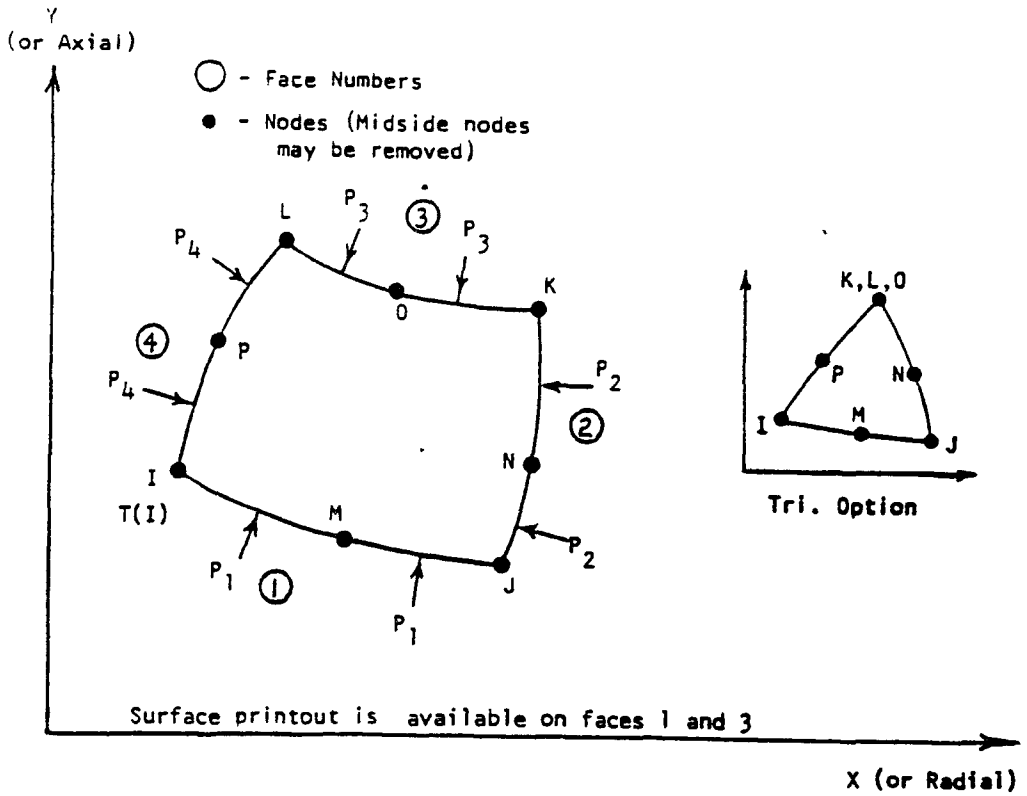

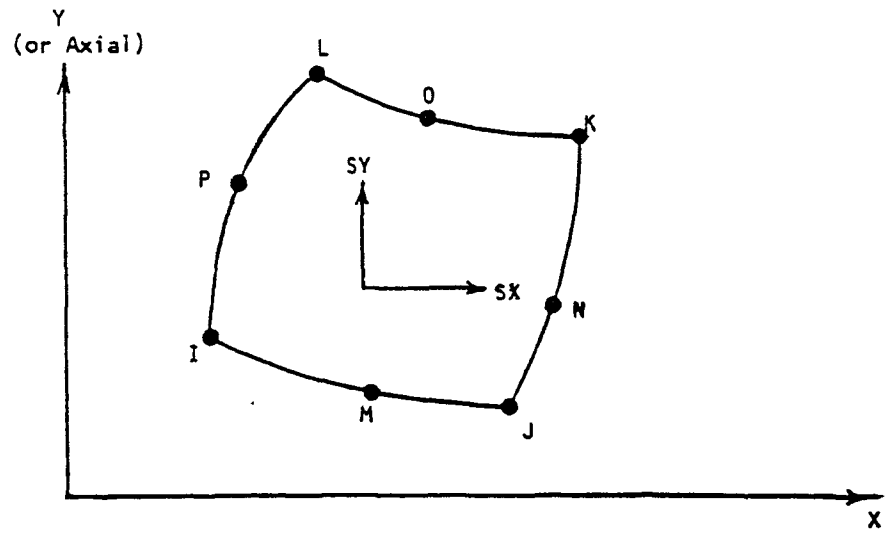

Figure 3.3: STIF 82 2-D 8-node element. (a) Geometry of the element (b) Element stress directions

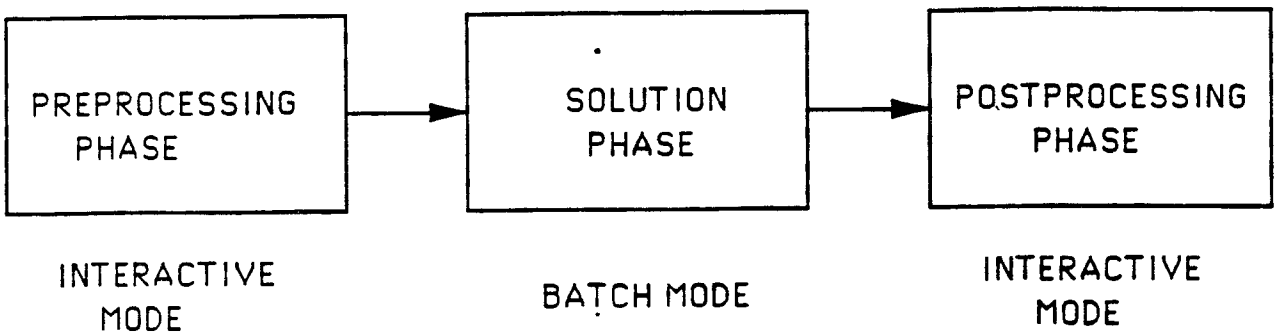

Figure 3.4: Modes of operation

(3) postprocessing

Preprocessing is the set of input lines related to defining a model and associated boundary conditions is given in this program. Once the preprocessing phase has been completed the user may progress through various analysis(same model) in solution phase. Finally the postprocessing operation is done, which analyse the solution data.

ANSYS program supports two modes: (1) Interactive (2) batch. The pre and post processing is done most efficiently in interactive mode and solution is carried out in batch mode as shown in Fig. 3.4. This software supports the graphics to view the geometry, displacement, deformed shape , and nodal stresses and the stress variation along the depth of the beam.

3.6.1 Preprocessing

For the simulation purpose static analysis is used. The static (KAN=0) analysis is used to solve for the displacement, stresses, strains and forces in structures under the action of applied loads. The result shows the displacements and the stress analysis of the diaphragm structure. In a preprocessing process a uniformly distributed load is applied to a span of $600\mu m$. In order to see the variation of stress along the

depth of the beam diaphragm structure it would be necessary to use 2-dimensional elements. In our case STIF 82 2-dimensional elements are used.

3.6.2 Solution Phase

In solution phase, element stiffness matrices for all elements are assembled to form structure stiffness matrix. Rows and columns corresponding to known displacement are eliminated before solution of simultaneous equations.

The relationship,

$[K][D] = [F]$

is then solved for unknown displacement matrix [D] according to

$[D] = [K]^{-1}[F]$ where [K]= structure stiffness matrix.

and [F]=structure force matrix.

For inverting [K] frontal technique is used. This mode is carried out in batch mode.

3.6.3 Post Processing

The strains are calculated from displacement and stresses are calculated from strains using concept of theory of elasticity. With the help of ANSYS graphics the stresses and deformed geometries of the beam diaphragm structure can be viewed. The input and output file for the beam diaphragm structure with square diaphragm of size $600 \times 600\mu m$ and a $10\mu m$ thickness is given in the appendix.

Chapter 4

Simulation Results

4.1 Results of ANSYS Simulations

The beam diaphragm structure consists of a thin square diaphragm with two rigid bosses as shown in Fig. 2.7. The density of elements is higher in the thin sensitive regions of the diaphragms, in order to get the exact location of the highest stress points. The applied pressure on a diaphragm creates in plane local bending moments proportional to local displacement and related curvature which, in turn, generates in plane tensile and compressive stresses. For positive pressure normal to a given surface, bending tensile stresses are near the diaphragm edges, while the bending compressive stresses are created at the diaphragm center which are shown in fig. 4.3 and 4.4. These are the location of stress sensing elements.

The presence of the rigid bosses on diaphragm causes the thin regions to withstand relatively high curvature, resulting in high bending moments and stresses in the thin film regions. The geometry of a double boss structure can be designed to give tensile and compressive stresses of equal magnitude, a property highly desirable for piezoresistive devices. Here the values of tensile stress is $570 kg/mm^2$ and compressive stress is $617 kg/mm^2$ which are very close. The edges of the suspended beam diaphragm structure were considered to be clamped edges and the boundary

conditions were fixed at the film edges for zero degree of freedom. The following figures describes the stress analysis, location of piezoresistors and sensitivity of the structure.

Fig. 4.1 is the ANSYS output which shows how the nodes and elements are generated in the beam diaphragm structure. The elements are shown by different colors.

The ANSYS output under the application of load from the top is given in fig. 4.2. The value of applied pressure at which the bosses touches the bottom is $1.3kg/mm^2$. The red color indicates the maximum tensile stress which is $570kg/mm^2$, where as blue color indicates the compressive stress which is $-617kg/mm^2$. Fig. 4.3 and 4.4 are the magnified views of these stresses.

Fig. 4.5 shows the deformed shape of the beam diaphragm structure after the application of pressure. The dotted line shows the original position of the structure.

Fig. 4.6 has the bar graph for the stress distribution along the lateral surface. The X axis has number of nodes along the surface where as Y axis has stress values. The maximum and minimum stress point location are clearly determined from this bar graph.

Fig. 4.7 explains how the overpressure protection is obtained for the beam diaphragm structure. The simulation was carried out with three values of the gap between the bosses and silicon bottom(clearance). The values are $10\mu m$, $15\mu m$, and $22\mu m$. Initially as the pressure increases the diaphragm deflection is linear. When the bosses touches the silicon bottom, it stops deflecting, but diaphragm still continues to withstand the pressure till the breaking stress point is reached. The diaphragm with $22\mu m$ gap has good linearity and it touches the bottom exactly when the stress reaches to yield point.

The values of tensile and compressive stresses are plotted against the pressure in

Fig. 4.8. As the values of the pressure increases, the tensile stress increases linearly where as compressive stress decreases and is opposite in magnitude.

4.2 Load Deflection Behavior

In this section FEM is used to simulate the beam diaphragm structure with different thicknesses. The ANSYS program input data for the beam diaphragm structure is given in appendix. The pressure deflection data obtained from the output file is used to plot the pressure versus deflection curves. The residual stress is also evaluated from the P/d versus d^2 curve. The procedure of evaluating it is as follows:

(1) Assume material properties of the structure as input to FEM.

(2) Obtain FEM results as a set of pressure deflection data.

(3) Plot the FEM pressure deflection data(P/d versus d^2) and obtain the values of slope and the intercept.

Fig. 4.9 shows the typical results of the pressure versus deflection. From analytical model

$$\frac{Pa^2}{(h+H)d} = C_2(\nu)\,(\frac{E}{1-\nu})\,(\frac{1}{a^2})\,d^2 + C_1\sigma_0 \qquad (4.1)$$

Fig. 4.10 shows the FEM pressure deflection results in a P/d versus d^2 plot. Since the material properties and geometries were already known (such as h, H, E, ν, and σ_0). The simulation was done using following properties.

$a = 300\mu m$, $E = 19,000 Kg/mm^2$, $\nu = 0.42$, $H = 5\mu m$, $h = 10\mu m$

The convenience of the expression Eq. 4.1 is the linear relationship between P/d and d^2. Hence biaxial modulus and residual stress can be determined by slope and intercept of the a plot P/d versus d^2.

From the fig. 4.10, the residual stress(intercept) is $\sigma_0 = 38$ kg/mm^2.

Above values are used as an input to FEM and the deflection and stress data are

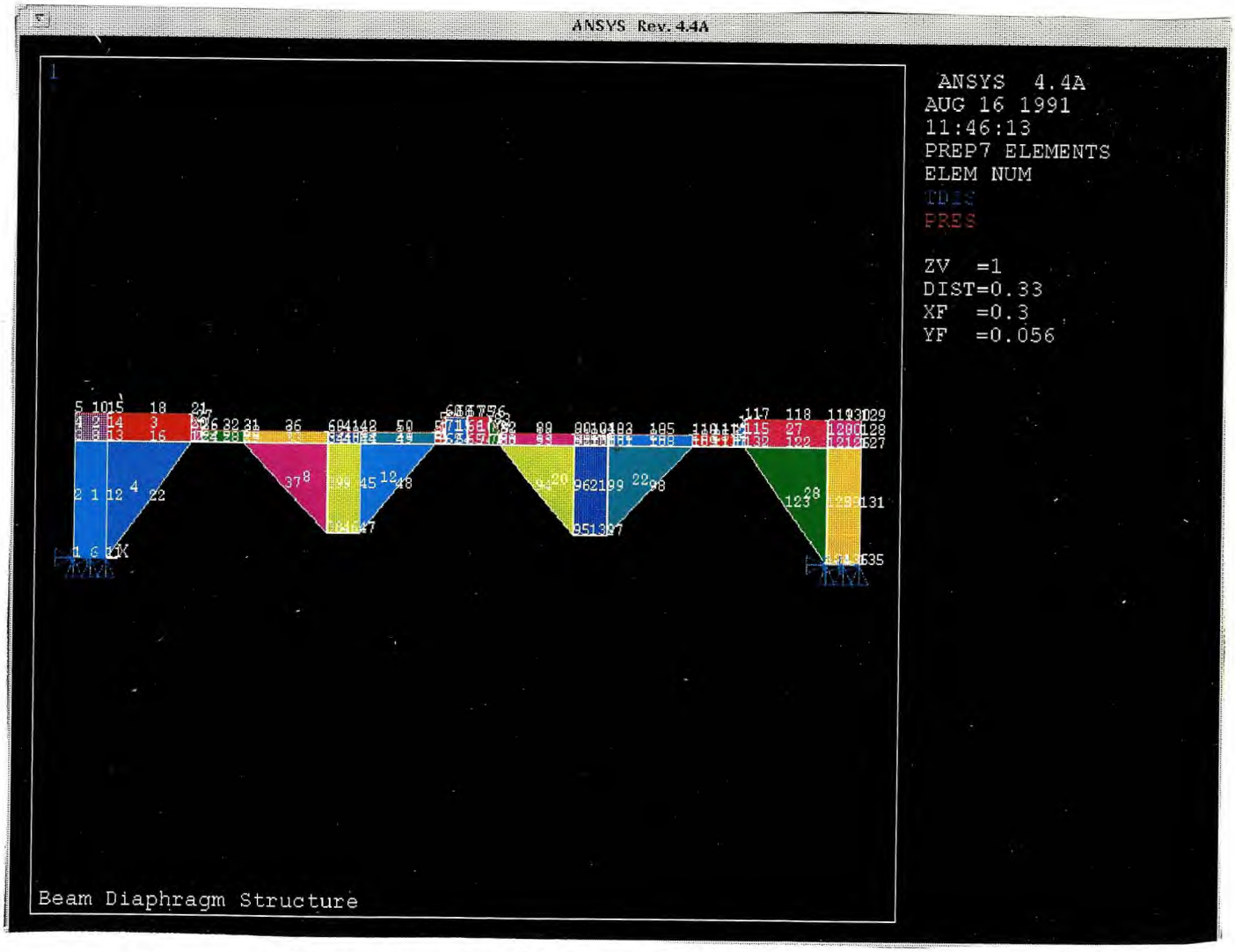

Figure 4.1: Finite Element Modeling of the beam diaphragm structure. Different color indicates the elements.

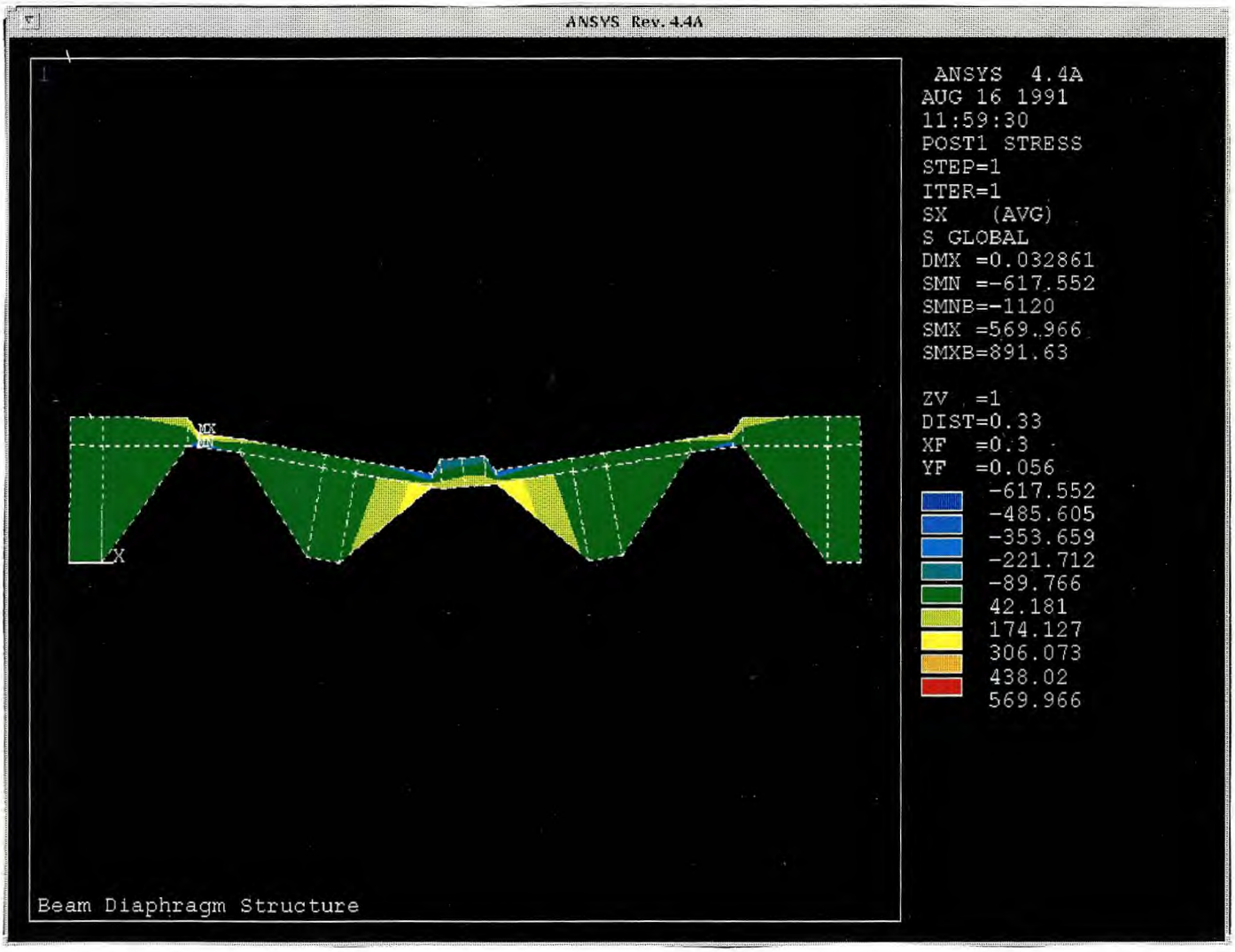

Figure 4.2: Stress distribution in beam diaphragm structure under the applied pressure. The different color indicates the average value of the stresses(SX).

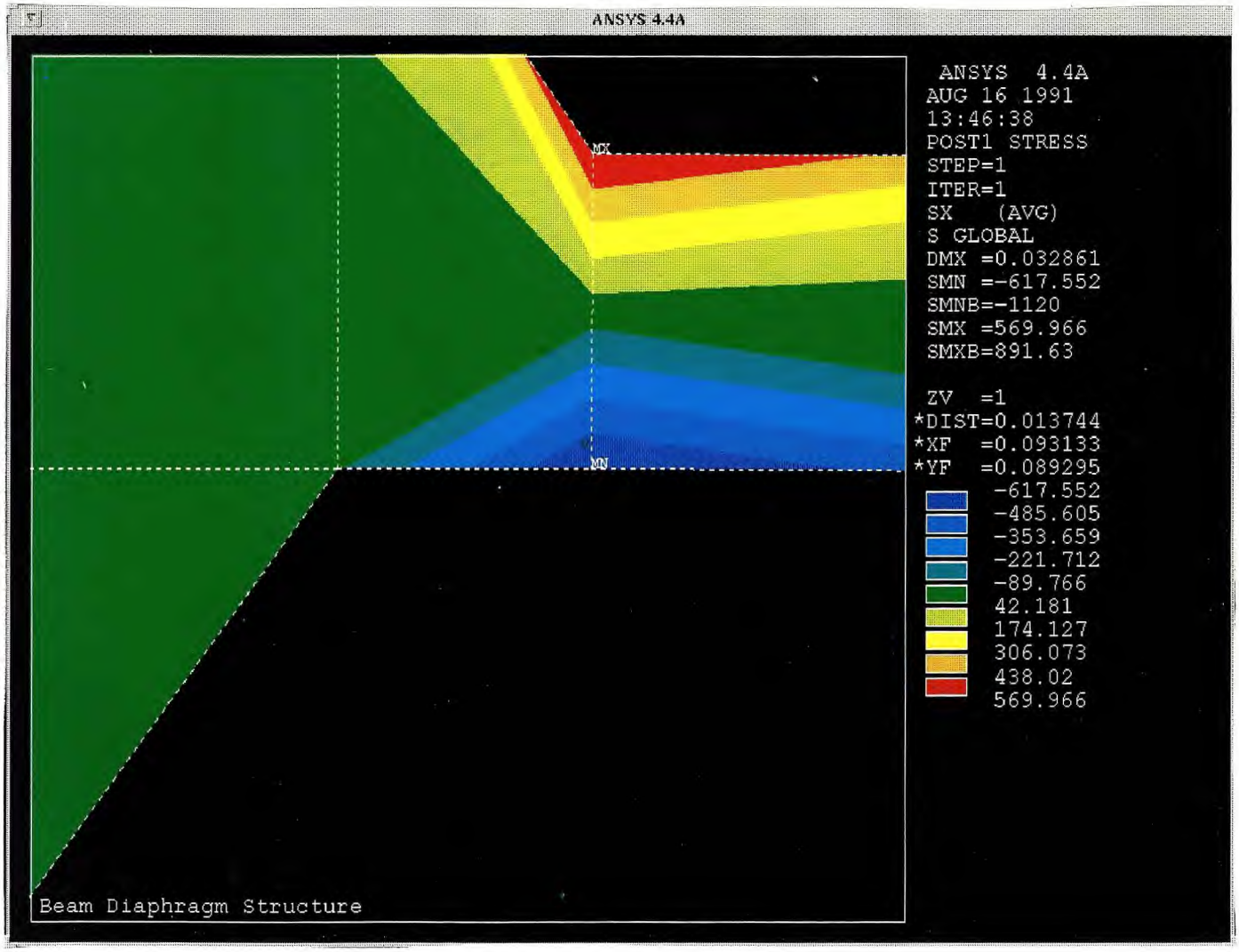

Figure 4.3: Magnified view of the tensile stress.

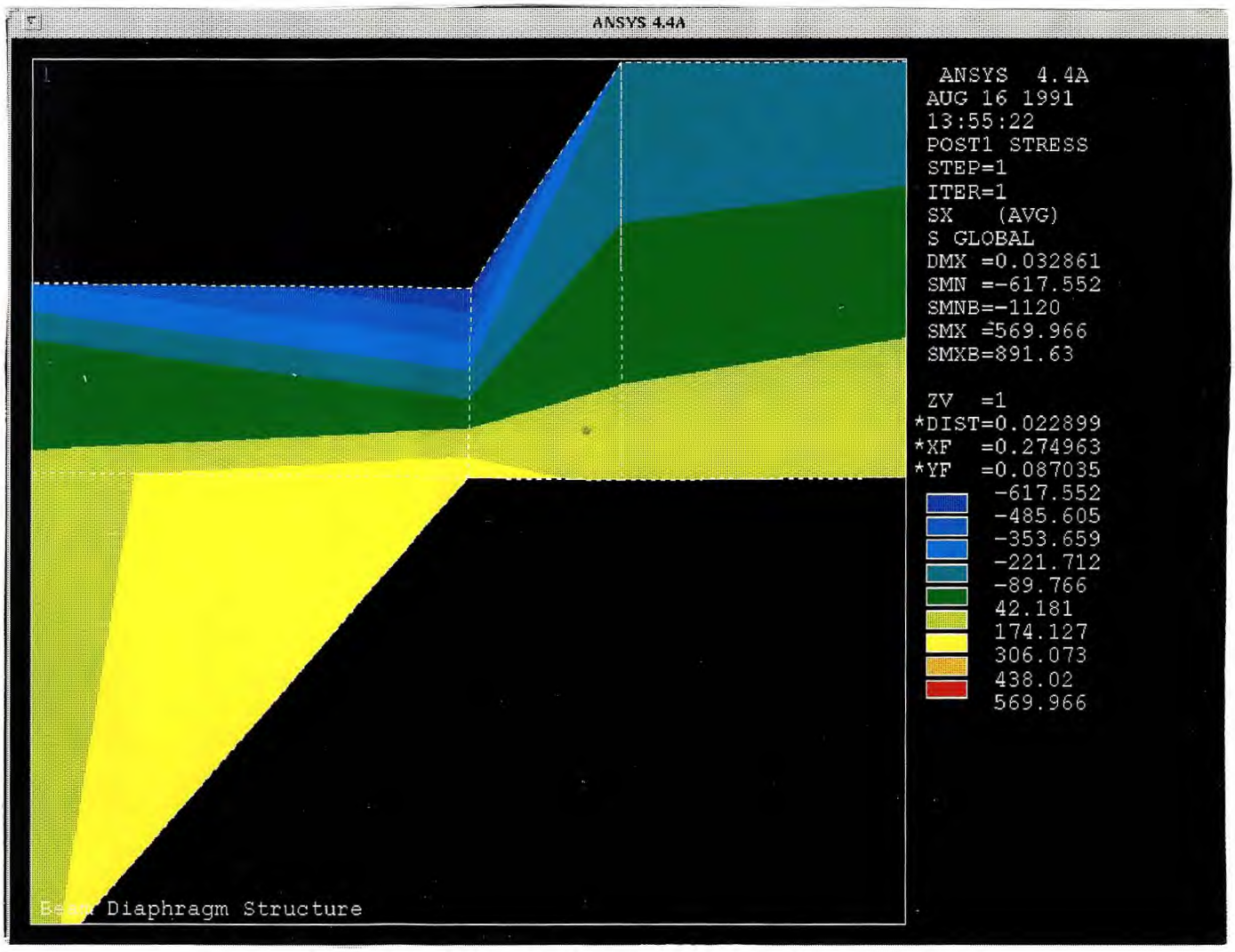

Figure 4.4: Magnified view of compressive stress.

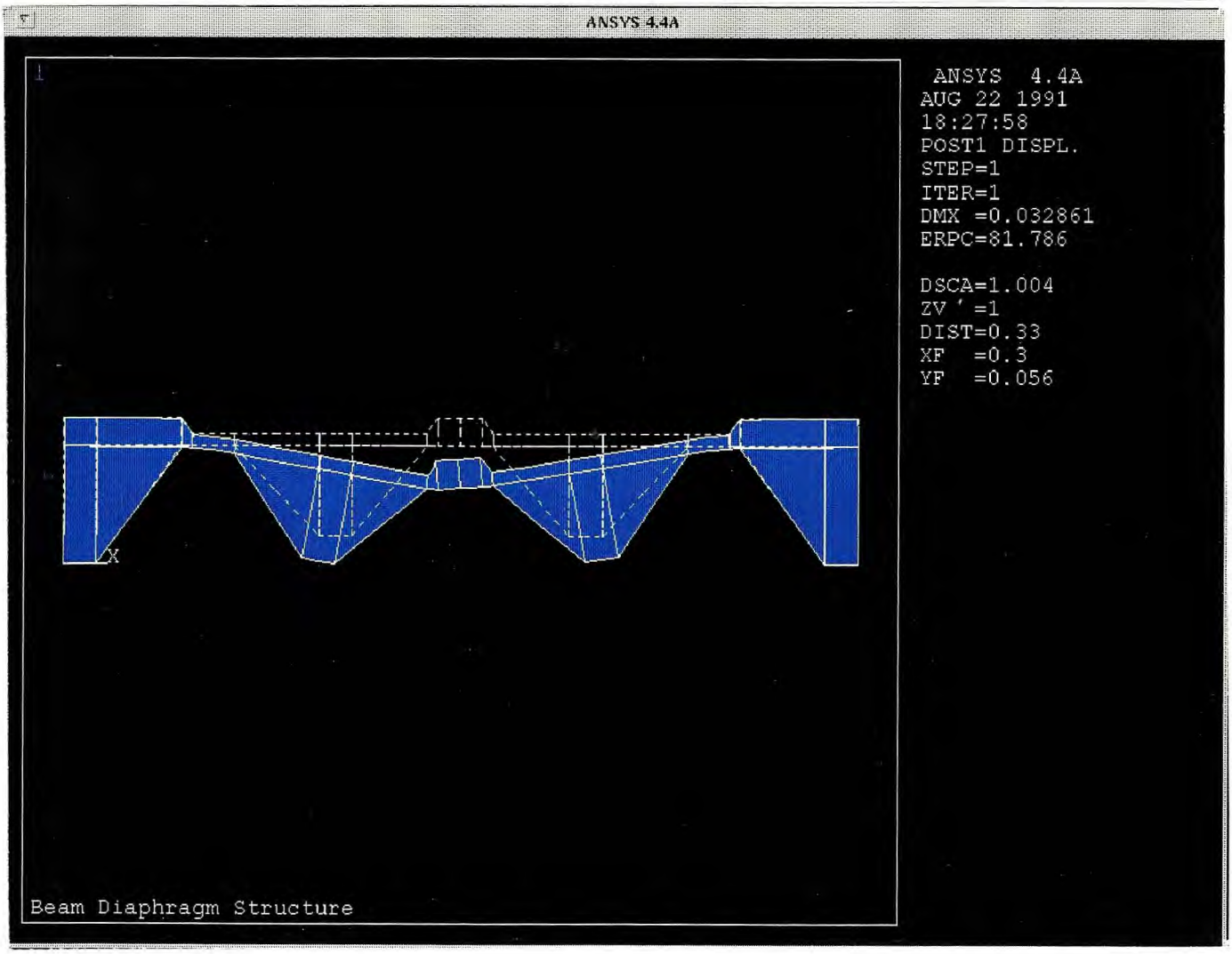

Figure 4.5: Deformation of beam diaphragm structure after the application of load.

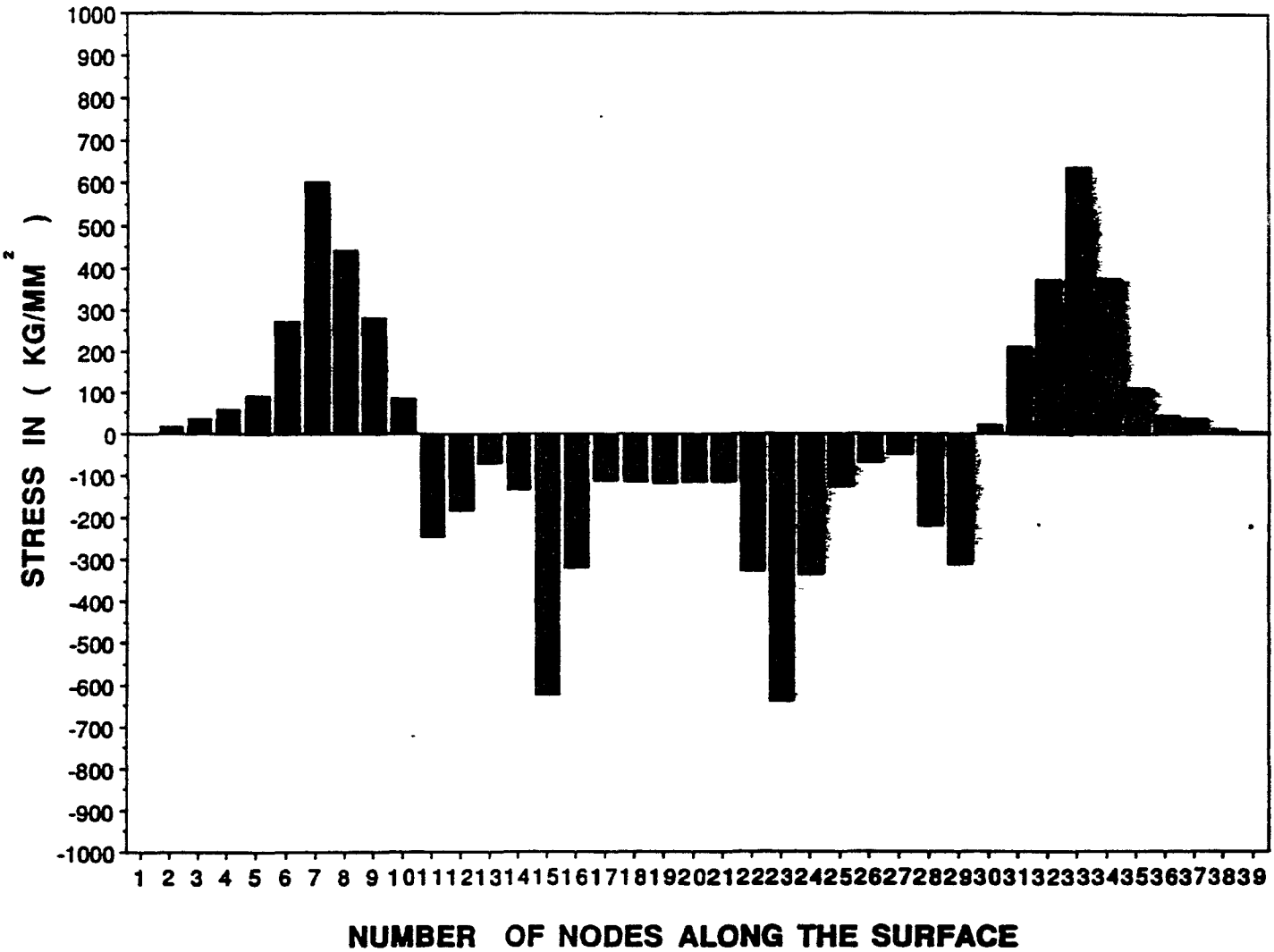

Figure 4.6: Stress distribution along the number of elements on the beam diaphragm structure.

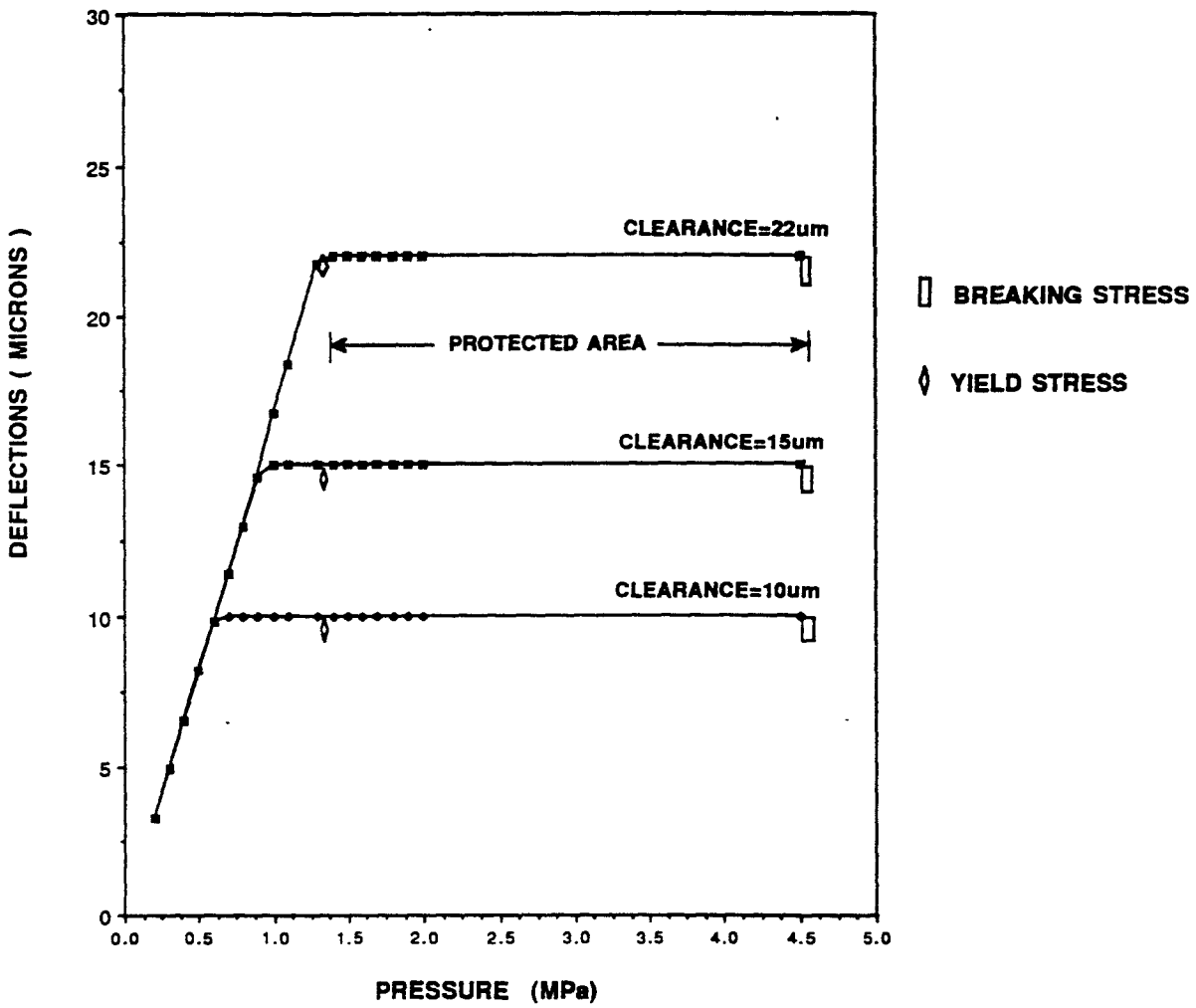

Figure 4.7: Over pressure protection for the beam diaphragm structure.

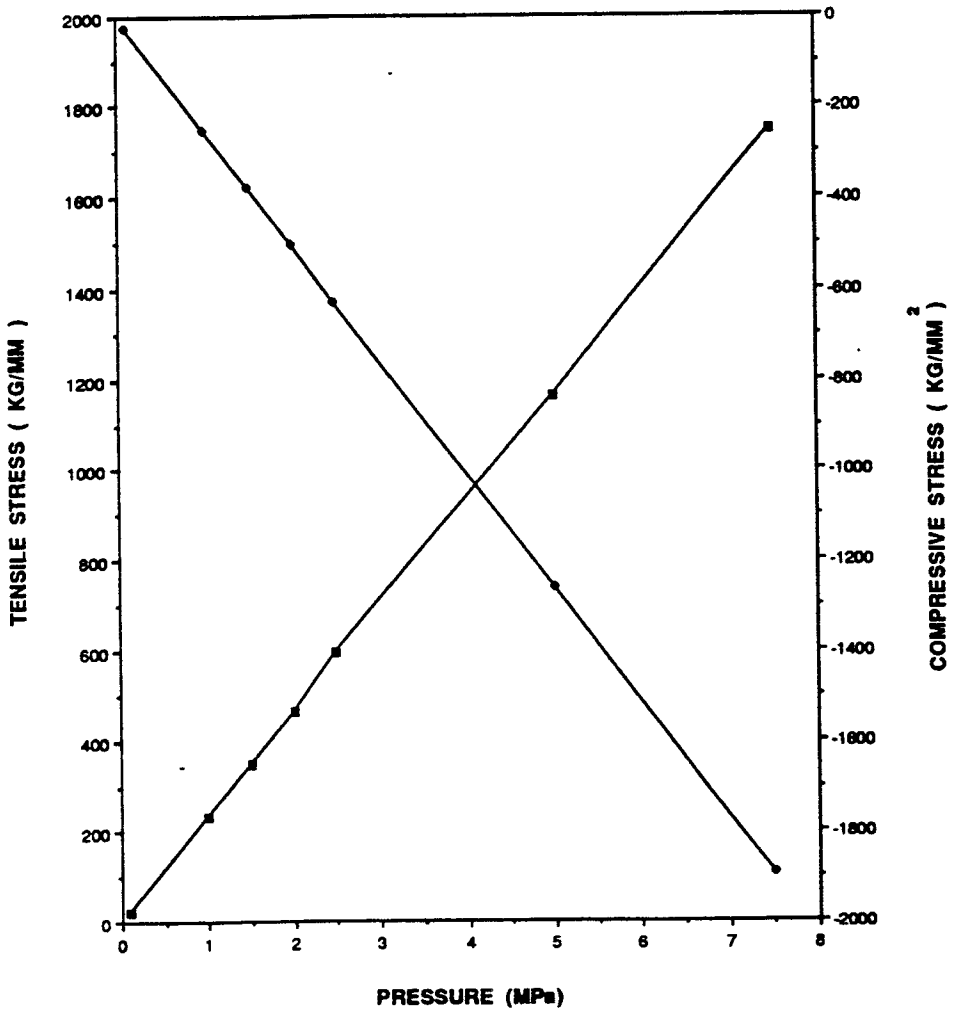

Figure 4.8: Pressure versus maximum/minimum stress curves.

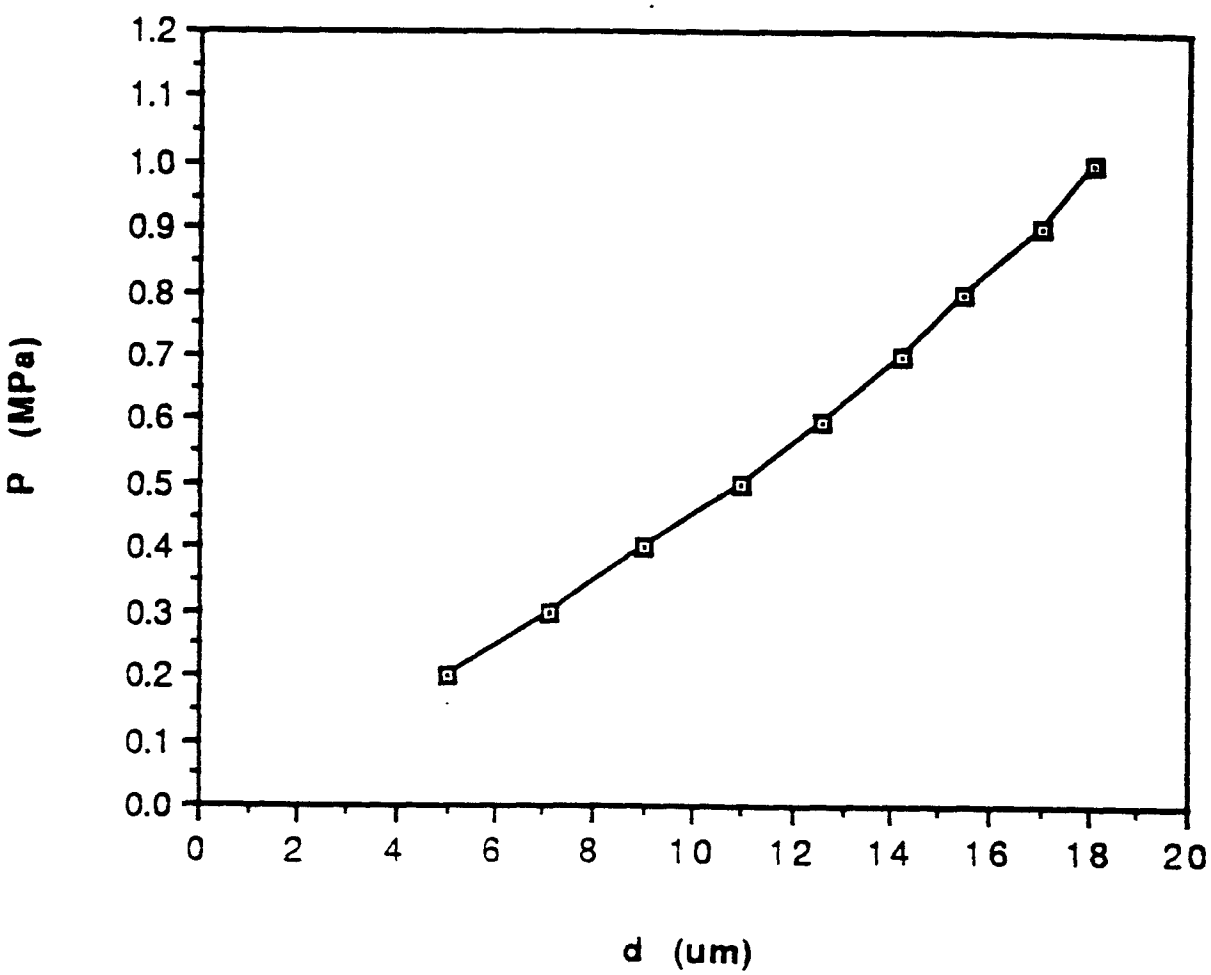

Figure 4.9: FEM results: pressure versus deflection curve.

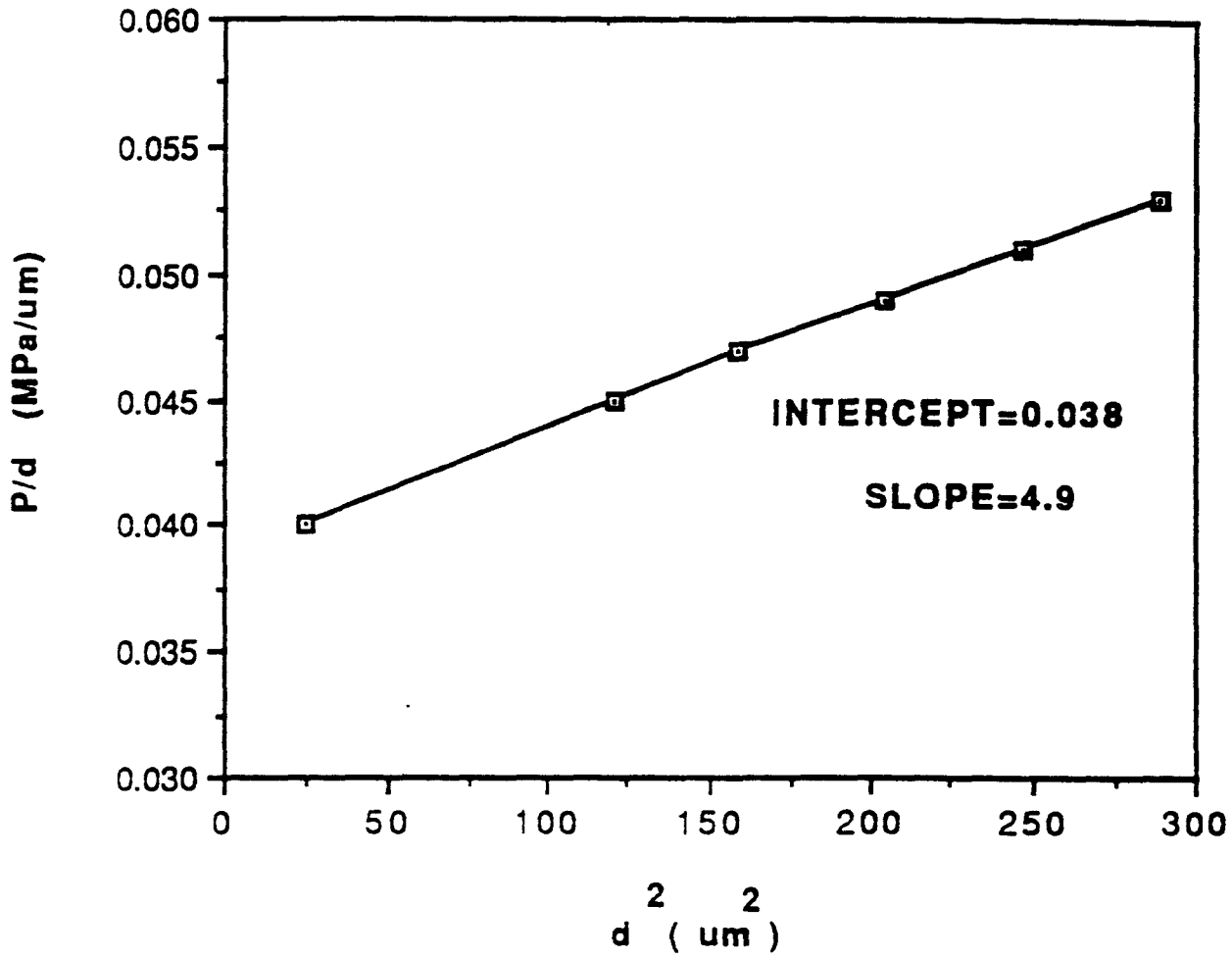

Figure 4.10: FEM results: P/d versus d^2 curve.

obtained from output file. Substituting the values of pressure or deflection in Eq. 4.1, results are varified with the FEM output.

Chapter 5

Design of Piezoresistive Pressure Sensor

5.1 Introduction

Four piezoresistive strain gage resistors are diffused in the diaphragm to form a fully active wheatstone bridge. The electrical output of the bridge is proportional to the input pressure. The outstanding mechanical [18] and electrical properties of a single crystal silicon make it ideal for these devices. It precisely returns to its original position after a deflection. High piezoresistive sensitivity, well defined electrical properties and lack of mechanical hysteresis are a few of the advantages of the single crystal silicon over other materials for pressure sensing applications.

5.2 Piezoresistance Coefficient

When silicon, either p or n type, is subjected to stress, causes a change in the resistivity. The change in resistance due to stress induced dimensional changes is depends on the amount of stress applied to it.

In semiconductors, the stress causes a change in the number of charge carriers. The stress S causes a volume change dV, which in turn causes a change dEg in the energy gap between the valence and conduction bands. Because of this, there is a change in number of carriers and therefore the resistivity changes. The fundamental piezoresistive coefficients of the crystal are denoted by π_{11}, π_{12} and π_{44} [20]. The coefficient π_{11} is called as the longitudinal piezoresistance coefficient, and $\pi_{12,}$ is referred to as transverse coefficient. π_{12} gives resistance change in the longitudinal direction to the stresses in the transverse direction. Besides these two coefficients, there are two simple shear coefficients, of which only one is exceptionally large. This is denoted by π_{44}. The approximate values of the coefficients are listed in table 5.1. The piezoresitive coefficients are sensitive to several quantities which are as follows.

(1) Conductivity(p type or n type)

(2) Orientation

(3) Temperature

(4) Doping

Conventional processing is more compatible with p-type diffused resistors. The dependance of the piezoresistive coefficients on impurity concentration at given temperature is given in fig. 5.1 and 5.2. P(N, T) is the piezoresistance factor and is a function of fermi integral. The above graphs are plotted as the function of impurity concentration ranging from 10^{16} to 10^{20} cm^{-3} and the temperature is ranging from -75 to 175^0C with 25^0C interval. In addition the piezoresistive factor

MATERIAL	RESISTIVITY (ohm-cm)	$\pi 11$	$\pi 12$	$\pi 44$
		10^{-12} (cm^2/dyne)		
n-Ge	~1			-138
p-Ge	~1			-97
n-Si	~12	-102	-53	
p-Si	~8	3	-1	+138

Table 5.1: Approximate piezoresistance coefficients at room temperature [Ref. 19]

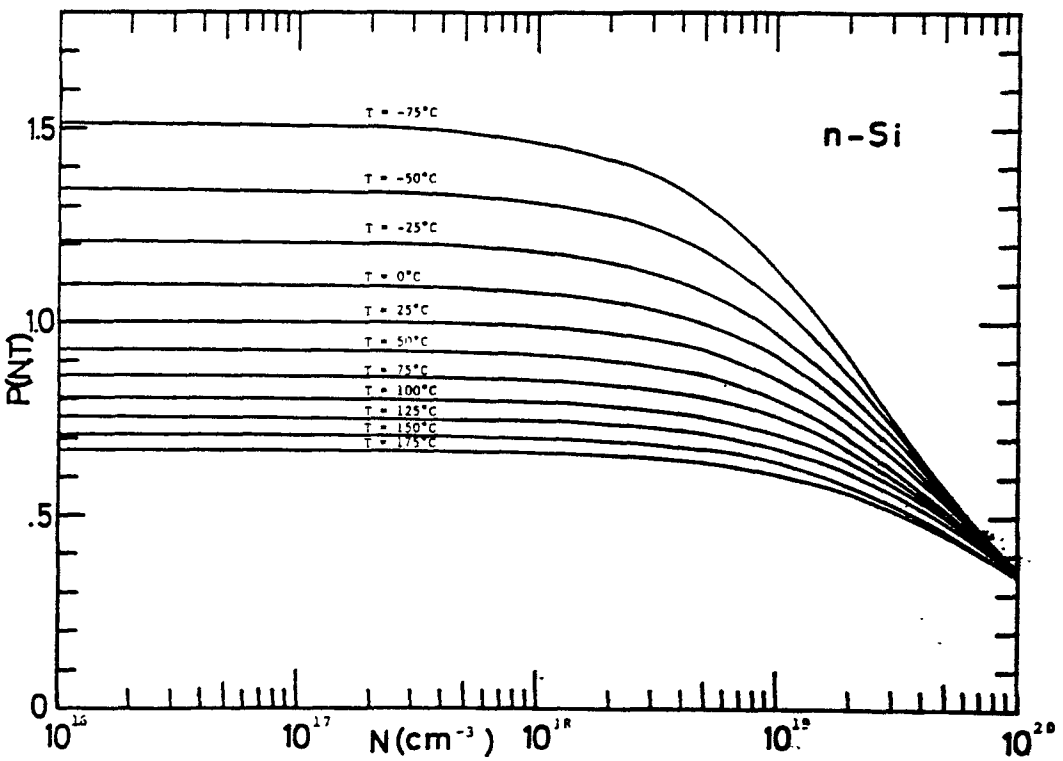

Figure 5.1: Piezoresistance factor P(N,T) as a function of impurity concentration and temperature for n-Si. [Ref. 24]

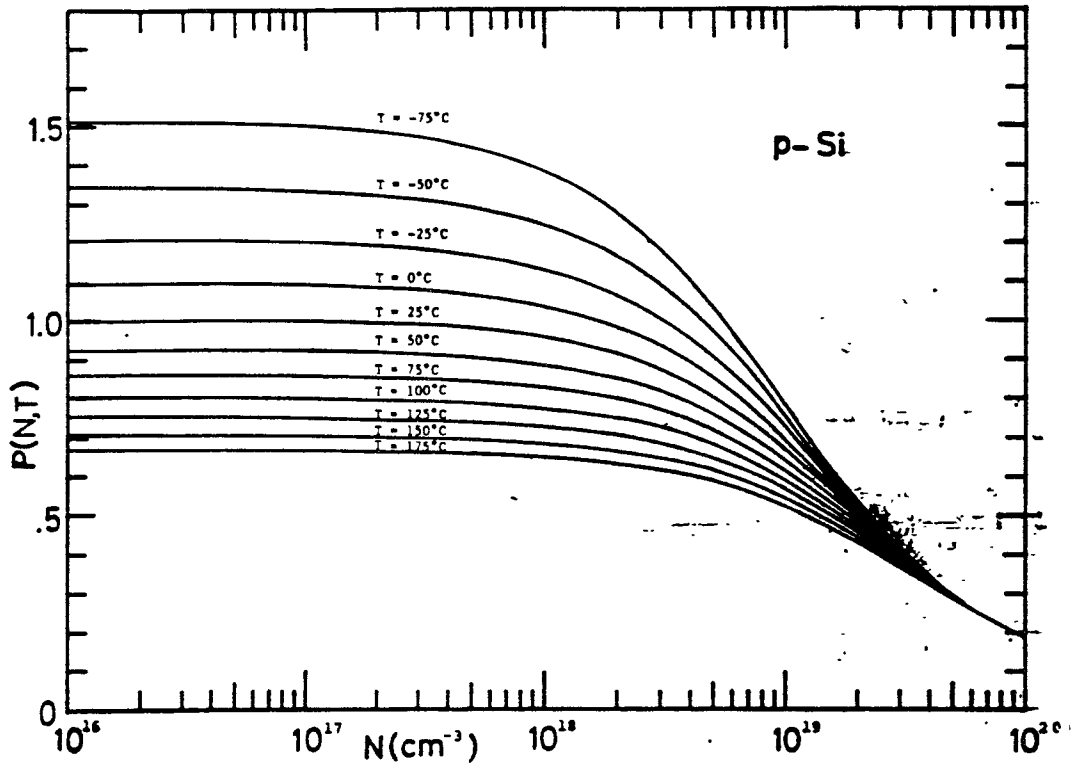

Figure 5.2: Piezoresistance factor P(N,T) as a function of impurity concentration and temperature for p-Si. [Ref. 24]

also depands on the crystal orientation. [24].

5.3 Piezoresistive Beam Diaphragm Structure

The design of the diaphragm and piezoresistors plays an essential part in the sensor performance. Normally, four resistors on a [100] silicon diaphragm are used for a silicon IC piezoresistive pressure sensor. In silicon diffused piezoresistive diaphragms the strip of low resistivity material is formed by impurity diffusion. These strip then function as electrical resistance stress gauges such that when diaphragm is deformed by a differential pressure, the resistance of the diffused strip changes in response. This is an "integrated beam diaphragm". Since the electrical resistance gauge is an integral part of the diaphragm, i. e. strip is not bonded to the diaphragm.

The piezoresistive coefficient relates the fractional change in resistance to the applied stress. For a diffused resistor subjected to parallel and perpendicular stress

components $\sigma_{||}$ and $\sigma_{\perp}$, respectively , the resistance change [4] is

$$(\frac{\Delta R}{R}) = \pi_{||}\sigma_{||} + \pi_{\perp}\sigma_{\perp} \tag{5.1}$$

Where $\pi_{||}$ and $\pi_{\perp}$ are piezoresistive coefficients parallel and perpendicular to the resistor length. Stresses applied to the resistor in longitudinal and transverse direction are $\sigma_{||}$ and $\sigma_{\perp}$ respectively. R is initial resistance with no applied stress and ΔR is the resistance variation. The magnitude of π_{44} varies from $138 \times 10^{-12} cm^2/dyne$ to $80 \times 10^{-12} cm^2/dyne$ in bulk material. The measured value [4] of π_{44} is $79 \times 10^{-12} cm^2/dyne$ is used here. Commonly used values for π_{11} and π_{44} are $3 \times 10^{-12} cm^2/dyne$ and -1 $\times 10^{-12} cm^2/dyne$, respectively.

In the [100] directions, the parallel and perpendicular piezoresistive coefficients are given by

$$\pi_{||} = \pi_{11} - 2(\pi_{11} - \pi_{12} - \pi_{44})(1/4) \tag{5.2}$$

$$= 40.5 \times 10^{-12} cm^2/dyn \text{ and}$$

$$\pi_{\perp} = \pi_{12} + (\pi_{11} - \pi_{12} - \pi_{44})(1/2) \tag{5.3}$$

$$= -38.5 \times 10^{-12} cm^2/dyn$$

Hence resistance oriented parallel and perpendicular to [100]diaphragm edge, the resistance change will be opposite and nearly equal. By making a full bridge , the temperature coefficients of the individual resistors are eliminated in the differential bridge output voltage.

5.4 Size of Resistors

In any real device, resistor size represents a tradeoff between reproducibility, which improves as the resistor size increases, and pressure sensitivity, which decreases with

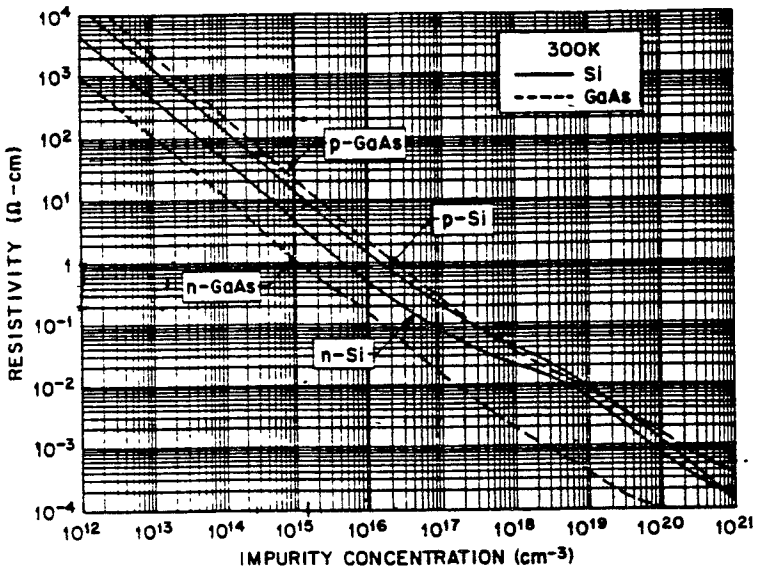

Figure 5.3: Resistivity change with impurity concentration. [Ref.21]

resistor size due to stress averaging effects in the finite resistor dimensions.

$$R = R_0(L/W) \tag{5.4}$$

where R=value of the resistor in Ω

R_0=sheet resistivity

L and W are the length and width of the diffused resistor. The sheet resistivity,

$$R_0 = \rho/t \tag{5.5}$$

where ρ is the resistivity of diffused p layer and t is the thickness. For p type Si and impurity doping of $5 \times 10^{19} cm^{-3}$, the resistivity can be found from the fig. 5.3.

$R_0 = 10\Omega \; for \; t = 2\mu m.$

Every resistor has a finite size and shape. For maximum sensitivity, the resistor length should be within 10 percent of the diaphragm width. For resistor of 150ohms value, using Eq. 5.4,

$150 = 10 \times (L/W)$

Thus, (L/W)=15.

DOPING (cm^{-3})	RESISTIVITY (ohm-cm) P-Si	SHEET RESISTIVITY (ohm / sq.)	L/W
1×10^{18}	2×10^{-2}	100	1.5
5×10^{18}	10^{-2}	50	3
1×10^{19}	8×10^{-3}	40	3.75
5×10^{19}	2×10^{-3}	10	15
8×10^{19}	10^{-3}	5	25

Table 5.2: Resistivity change with impurity concentration

For W=5μm, L=75μm.

Table 5.2 shows the values of the R_0 and L/W with doping variations.

5.5 Sensitivity

Table 5.3 shows the values of the longitudinal and transverse stresses obtained from the finite element method. Using the Eq. 5.1, 5.2, and 5.3,

$$(\frac{\Delta R}{R})_{\parallel} = \pi_{\parallel}\sigma_{\parallel} + \pi_{\perp}\sigma_{\perp} = \alpha = 2.35/mm\ of\ Hg \tag{5.6}$$

$$(\frac{\Delta R}{R})_{\perp} = \pi_{\perp}\sigma_{\parallel} + \pi_{\parallel}\sigma_{\perp} = \beta = 2.47/mm\ of\ Hg \tag{5.7}$$

For a full bridge having differential output voltage and an applied supply voltage of V_{cc}, the bridge output is

$$S = \frac{\Delta V}{V_{cc}} = \frac{\beta - \alpha}{2 + \alpha + \beta} = 2.56\ V/V \bullet mm\ of\ Hg \tag{5.8}$$

which is the sensitivity of the beam diaphragm structure. Fig. 5.4 shows the variation of sensitivity with different location of resistors.

DISTANCE FROM THE CENTER (μM)	$\sigma_{\parallel}$ Kg/mm^2	$\sigma_{\perp}$ Kg/mm^2	SENSITIVITY V/V mm of Hg
160	153	26	0.482
185	388	19	1.375
211	623	12.1	2.56
236	316	15	1.249

Table 5.3: Values of sensitivity with different location of the resistors.

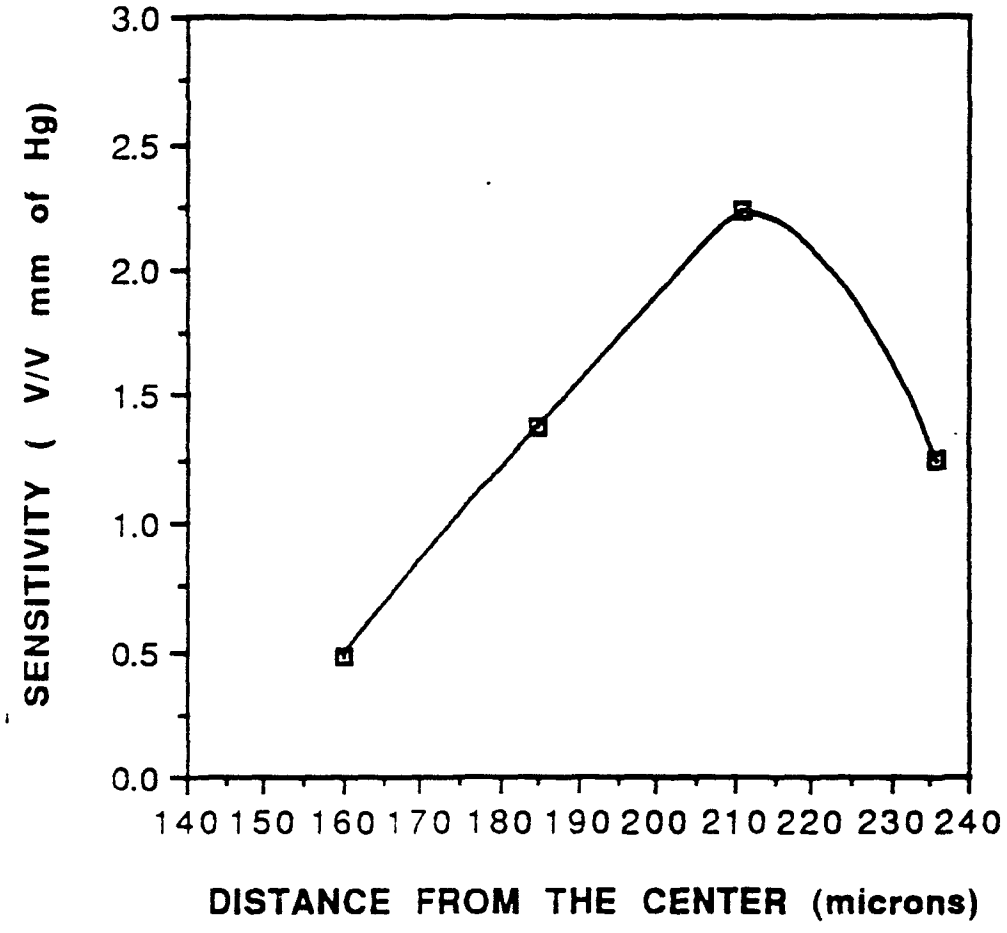

Figure 5.4: Variation of sensitivity with different location of resistors.

pressure for which the diaphragm senses is 3 kpa. Therefore the linear range of operation is 3 Kpa to 1.4 Mpa(2000psi).

5.6 Micromachining Process

It has become common practice to group under the title of "micro-machining" all the processes of the type and used in microelectronics but more specifically used to manufacture three dimensional micro-mechanical components. The strength of this technique lies in the systematic use of 'batch processing', the physical and chemical process, with well known advantages;

- Very low production cost.
- No theoretical limit to the possible miniaturization.
- Very precise control of material structure and composition.
- Use of small quantities of material, which can be rare or pure.
- The only possible method that can provide access to some physical phenomena(elastic limit of single crystals, field effect etc.).

Two major categories of micromachining techniques have been developed: orientation dependent chemical etching of the crystalline silicon substrate (bulk micromachining), and selective chemical etching of the multilayer depositions of thin films(surface micromachining).

5.6.1 Bulk Micromachining

The first micromachined device, a silicon diffused element piezoresistive diaphragm was fabricated using bulk technology. This technology has evolved over two decades and as a result of which it has been used extensively to fabricate complex micromachined structures. As noted earlier, this technique involves anisotropic etching of the silicon substrate. Several orientation dependent etchants such as KOH(potassium

hydroxide), EDP(ethlene diamine-pyrocatechol) and hydrezine etch heavily boron doped silicon very slowly. This property has been exploited to make a variety of micromechanical structures, such as diaphragms, cantilever beams and recording probes for neuro-physiology. KOH is used in near saturated solutions(1:1 in water by weight) at 85^0C to produce a uniform etch and bright surface. Usually this type of etch is preferred for shallow cavities where uniformity is important. It attacks silicon dioxide at a rate of about $60A^0$/min. EDP is better suited for deep etching since its oxide etch is negligible($5A^0$/min). Hydrazine has the advantage of not etching aluminium but it has other disadvantages such as: it tends to produce rough surfaces and is very dangerous to handle.

In terms of verticle depth control, the boron etchstop technique has been developed to allow the etching process to stop at desired depth. This process relies on the fact that EDP stops etching when the boron impurity concentration exceeds about $5 \times 10^{19} cm^{-3}$ in the silicon lattice.

The main disadvantatge of the bulk technology is non-compability with the conventional IC processing. The main problem is the etch rate of anisotropic etching. They are very slow unless they are heated upto certain temperature ($85^0C - 115^0C$). A typical etch rate for KOH at 85^0C is $1\mu m$/min [22]. Boron etch stop involves high level doping which introduces another problem. The high concentration doping will prelude the formation of electronic circuitry. If the devices are formed in epitaxial material grown on the top of the etch stop layer(a boron buried layer), there are problem with epitaxial film quality and out- diffusion of boron from the buried layer. For the fabrication of beam diaphragm structure the anisotropic etching can be used for the two bosses from the back. So the bulk micromachining technique is recommended.

5.6.2 Surface Micromachining

The second approach, surface micromachining, utilizes the selective etching of thin film sandwiches. A sacrificial layer used to offset the structural film from the substrate and is later removed using a selective chemical etchant. Although originally demonstrated with metal films[23], this process has been primarily for fabrication of polycrystalline silicon(polysilicon) microstructures.

Recently, the surface micromachining technology is drawing more attention because this technology avoids some challenging processing difficulties of bulk technology, provides better compatability with standard silicon device fabrication sequence and offers new degree of freedom for the design of integrated sensors, actuators and circuits. The main advantage of this technology is that we can fabricate free standing polysilicon microstructures by removing the oxide layer on which they are formed by hydrofluric acid(HF) etching. Using this technology, various type of structures such as rotating and sliding structures, gears, springs and various applications such as cross point switching array have been made.

5.6.3 Proposed Micromachining Process

The process for the fabrication of beam diaphragm structure is suggested [14] here. Figure 5.5 shows the schematic of the process. The [100] n-type silicon wafer is the starting material(Fig. 5.5a). The wafer is subjected to a cleaning procedure to remove any organic and inorganic residues from the surfaces. The heavily boron doped layer(P^+ Si) can be formed on the surface of Si wafer by diffusion process(Fig. 5.5b). Then approximately 1 μm silicon dioxide is grown in(Fig. 5.5c) an oxidation oven.

A silicon oxide "window" is open on the backside of wafer by photolithographic techniques(Fig. 5.5d). Using an anisotropic etching on the [100] surface of the

silicon wafers, the edges of the window created along [110] plane. The wafer is then subjected to an etching solution which etches silicon fast but slows down at the p^+ Si layer(Fig. 5.5e). The etching can be done by using 20 percent KOH aqueous solution at 50^0C. Then the silicon dioxide is removed (Fig. 5.5f). It is well known that the high concentration of boron in silicon slows down the etching rate significantly for many chemical etchants. The fig. 5.5g explains how the diaphragm structure can be etch from the top. The beams can be formed by EPW etching [25]. Then the p-type piezoresistors are made on the beam by ion implantation.

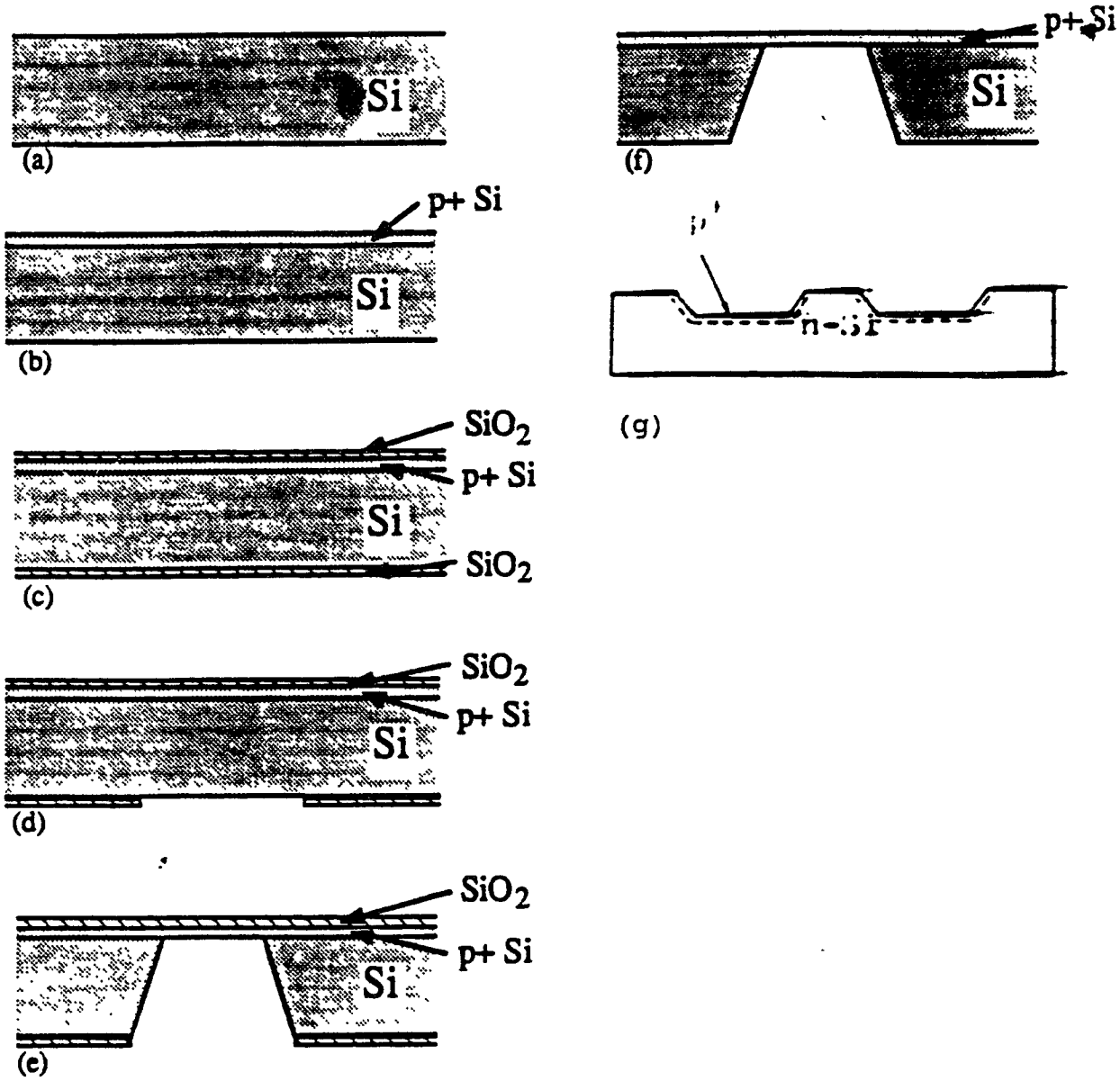

Figure 5.5: Proposed Micromachining Process

Chapter 6

Conclusion

As discussed in the previous chapters, the design consists of a beam diaphragm structure, piezoresistive coefficients and resistors. This type of structure can be used for pressure sensor in industrial and automobile applications.

This work has been successfully simulated using finite element method. Here, the single crystal silicon is used for the microstructure because of the known properties and high mechanical strength. The proposed design can be fabricated using micromachining technology as described in the previous chapters. The load deflection behavior of the beam diaphragm structure is derived using mathematical formula. The values of the pressure and deflection in the mathematical model are again calculated using FEM results and verified.

The stress distribution illustrated by above chapters provides the basis for understanding present sensors and trade offs necessary in their design and processing.

Further they offer a starting point for the creation of new designs. The arrangement would maximize pressure sensitivity while minimizing the effects of nonlinearity. The beam diaphragm structure with different clearance of the bosses with silicon bottom and thicknesses were simulated by ANSYS program. This program gives the stress distribution along the thickness of the diaphragm which gives the values of the stresses and it's location in the graphics mode. The following provides a summary of these benefits.

- The linear range of operation is 3 kpa to 1.4 Mpa.
- High pressure sensitivity by appropriate location of resistors.
- High pressure overload, i. e. 400 times overpressure protection is obtained.
- micromachining technique can be used for fabrication.

Appendix

ANSYS Output File

```
 THIS IS THE ANSYS(R) ENGINEERING ANALYSIS SYSTEM
 COPYRIGHT(C)  1971, 1978, 1982, 1983, 1985, 1987, 1989, 1990
 SWANSON ANALYSIS SYSTEMS, INC. AS AN UNPUBLISHED WORK.
 PROPRIETARY DATA - UNAUTHORIZED USE, DISTRIBUTION, OR DUPLICATION
 IS PROHIBITED.  ALL RIGHTS RESERVED.

 IF RUNNING INTERACTIVELY, ENTER  /INTER
1
                **********  ANSYS INPUT DATA LISTING (FILE18)  **********

     1   /prep7
     2   /title,Beam Diaphragm structure,clearance=22u
     3   ET,1,82
     4   KAN,0
     5   MP,EX,1,1.9E04
     6   n,1,0,0
     7   n,2,0,0.045
     8   n,3,0,.090
     9   n,4,0,.101
    10   n,5,0,.112
    11   n,6,.0125,0
    12   n,8,.0125,.09
    13   n,10,.0125,.112
    14   n,11,.025,0
    15   n,12,.025,.045
    16   n,13,.025,.090
    17   n,14,.025,.101
    18   n,15,.025,.112
    19   n,16,.057,.090
    20   n,18,.057,.112
    21   n,19,.089,.09
    22   n,20,.089,.101
    23   n,21,.089,.112
    24   n,22,.057,.045
    25   n,23,.093,.09
    26   n,24,.097,.09
    27   n,25,.097,.095
    28   n,26,.097,.1
    29   n,27,.093,.106
    30   n,28,.113,.09
    31   n,29,.129,.09
    32   n,30,.129,.095
    33   n,31,.129,.1
    34   n,32,.113,.1
    35   n,33,.161,.09
    36   n,34,.193,.09
    37   n,35,.193,.095
    38   n,36,.161,.1
    39   n,37,.161,.056
    40   n,38,.193,.022
    41   n,39,.193,.056
    42   n,40,.2055,.09
    43   n,41,.2055,.1
    44   n,42,.218,.1
    45   n,43,.218,.095
    46   n,44,.218,.09
    47   n,45,.218,.056
    48   n,46,.2055,.022
    49   n,47,.218,.022
    50   n,48,.2465,.056
    51   n,49,.2465,.09
    52   n,50,.2465,.1
    53   n,51,.275,.1
    54   n,52,.275,.095
    55   n,53,.275,.09
```

```
     56   n,59,.279,.106
     57   n,60,.283,.112
     58   n,61,.283,.106
     59   n,62,.283,.09
     60   n,63,.279,.09
1
                ********** ANSYS INPUT DATA LISTING (FILE18)  **********

     61   n,64,.2915,.09
     62   n,65,.3,.09
     63   n,66,.3,.101
     64   n,67,.3,.112
     65   n,68,.2915,.112
     66   n,69,.193,.1
     67   n,74,.3085,.09
     68   n,75,.3085,.112
     69   n,76,.317,.112
     70   n,77,.317,.101
     71   n,78,.317,.09
     72   n,79,.321,.09
     73   n,80,.325,.09
     74   n,81,.325,.095
     75   n,82,.325,.1
     76   n,83,.321,.106
     77   n,89,.3535,.1
     78   n,90,.382,.1
     79   n,91,.382,.095
     80   n,92,.382,.09
     81   n,93,.3535,.09
     82   n,94,.3535,.056
     83   n,95,.382,.022
     84   n,96,.382,.056
     85   n,97,.407,.022
     86   n,98,.439,.056
     87   n,99,.407,.056
     88   n,100,.3945,.09
     89   n,101,.407,.09
     90   n,102,.407,.095
     91   n,103,.407,.1
     92   n,104,.3945,.1
     93   n,105,.439,.1
     94   n,106,.507,.09
     95   n,107,.471,.095
     96   n,108,.439,.09
     97   n,109,.471,.09
     98   n,110,.471,.1
     99   n,111,.487,.1
    100   n,112,.503,.095
    101   n,113,.487,.09
    102   n,114,.503,.09
    103   n,115,.511,.101
    104   n,116,.507,.106
    105   n,117,.511,.112
    106   n,118,.543,.112
    107   n,119,.575,.112
    108   n,120,.575,.101
    109   n,121,.575,.09
    110   n,122,.543,.09
    111   n,123,.543,.045
    112   n,124,.575,0
    113   n,125,.575,.045
    114   n,126,.5875,.09
    115   n,127,.6,.09
    116   n,128,.6,.101
    117   n,129,.6,.112
    118   n,130,.5875,.112
```

```
    119   n,131,.6,.045
    120   n,132,.511,.09
1
                ***********  ANSYS INPUT DATA LISTING (FILE18)  ***********

    121   n,133,.503,.1
    122   n,134,.3945,.022
    123   n,136,.5875,0
    124   n,135,.6,0
    125   en,1,1,11,13,3,6,12,8,2
    126   en,2,3,13,15,5,8,14,10,4
    127   en,3,13,19,21,15,16,20,18,14
    128   en,4,19,13,11,11,16,12,11,22
    129   en,5,19,24,26,21,23,25,27,20
    130   en,6,24,29,31,26,28,30,32,25
    131   en,7,29,34,69,31,33,35,36,30
    132   en,8,34,29,38,38,33,37,38,39
    133   en,9,38,47,44,34,46,45,40,39
    134   en,10,34,44,42,69,40,43,41,35
    135   en,11,44,53,51,42,49,52,50,43
    136   en,12,53,44,47,47,49,45,47,48
    137   en,14,53,62,60,51,63,61,59,52
    138   en,15,62,65,67,60,64,66,68,71
    139   en,16,65,78,76,67,74,77,75,66
    140   en,17,78,80,82,76,79,81,83,77
    141   en,19,80,92,90,82,93,91,89,81
    142   en,20,92,80,95,95,93,94,95,96
    143   en,21,95,97,101,92,134,99,100,96
    144   en,22,109,101,97,97,108,99,97,98
    145   en,23,101,109,110,103,108,107,105,102
    146   en,24,92,101,103,90,100,102,104,91
    147   en,25,109,114,133,110,113,112,111,107
    148   en,26,114,132,117,133,106,115,116,112
    149   en,27,132,121,119,117,122,120,118,115
    150   en,28,121,132,124,124,122,123,124,125
    151   en,29,127,121,124,135,126,125,136,131
    152   en,30,121,127,129,119,126,128,130,120
    153   d,1,all
    154   d,6,all
    155   d,11,all
    156   d,124,all
    157   d,135,all
    158   d,136,all
    159   ep,2,3,1.3
    160   ep,3,3,1.3
    161   ep,5,3,1.3,,7,1
    162   ep,10,3,1.3,,11,1
    163   ep,13,3,1.3,,15,1
    164   ep,16,3,1.3,,19,1
    165   ep,23,3,1.3,,27,1
    166   ep,30,3,1.3
    167   ITER,1,1,1
    168   /PBC,ALL,1
    169   /PNUM,NODE,1
    170   /PNUM,ELEM,1
    171   nplot
    172   eplot
    173   AFWRITE
    174   FINISH
    175   /INPUT,27
    176   FINISH
    177   /POST1
    178   set,1,1
    179   GLOBAL,1
    180   PRESTR
1
```

```
   181   pldisp,1
   182   plnstr,sx
   183   finish
   184
   185
```

```
1           ANSYS - ENGINEERING ANALYSIS SYSTEM  REVISION 4.4      A 24   NEW JERS
      ANSYS(R)  COPYRIGHT(C) 1971, 1978, 1982, 1983, 1985, 1987, 1989, 1990   SWANS
      PROPRIETARY DATA - UNAUTHORIZED USE, DISTRIBUTION OR DUPLICATION IS PROHIBITE
      FOR SUPPORT CALL DAVID PEREL       PHONE (201) 596-3356    TWX

 TITLE
**UNIVERSITY VERSION FOR EDUCATIONAL PURPOSES ONLY**

         ***** ANSYS ANALYSIS DEFINITION (PREP7) *****

NEW TITLE= Beam Diaphragm structure,clearance=22u


ELEMENT TYPE  1 USES STIF 82
 KEYOPT(1-9)=   0   0   0     0   0   0      0   0   0
 INOPR=  0  NUMBER OF NODES=   8

MULTI-NODE STRESS SOLID, 2-D

CURRENT NODAL DOF SET IS  UX    UY
 TWO-DIMENSIONAL STRUCTURE

ANALYSIS TYPE=  0   (STATIC ANALYSIS)

 MATERIAL   1          COEFFICIENTS OF EX   VS. TEMP EQUATION
  C0 =   19000.00

PROPERTY TABLE EX    MAT=   1  NUM. POINTS=  2
    TEMPERATURE     DATA    TEMPERATURE     DATA
     -9999.0       19000.      9999.0       19000.

NODE      1  KCS= 0  X,Y,Z=       0.           0.           0.

NODE      2  KCS= 0  X,Y,Z=       0.      0.45000E-01       0.

NODE      3  KCS= 0  X,Y,Z=       0.      0.90000E-01       0.

NODE      4  KCS= 0  X,Y,Z=       0.      0.10100           0.

NODE      5  KCS= 0  X,Y,Z=       0.      0.11200           0.

NODE      6  KCS= 0  X,Y,Z= 0.12500E-01       0.           0.

NODE      8  KCS= 0  X,Y,Z= 0.12500E-01 0.90000E-01       0.

NODE     10  KCS= 0  X,Y,Z= 0.12500E-01 0.11200           0.

NODE     11  KCS= 0  X,Y,Z= 0.25000E-01       0.           0.

NODE     12  KCS= 0  X,Y,Z= 0.25000E-01 0.45000E-01       0.

NODE     13  KCS= 0  X,Y,Z= 0.25000E-01 0.90000E-01       0.

NODE     14  KCS= 0  X,Y,Z= 0.25000E-01 0.10100           0.

NODE     15  KCS= 0  X,Y,Z= 0.25000E-01 0.11200           0.

NODE     16  KCS= 0  X,Y,Z= 0.57000E-01 0.90000E-01       0.
```

```
NODE    18  KCS= 0  X,Y,Z= 0.57000E-01 0.11200          0.
NODE    19  KCS= 0  X,Y,Z= 0.89000E-01 0.90000E-01      0.
NODE    20  KCS= 0  X,Y,Z= 0.89000E-01 0.10100          0.
NODE    21  KCS= 0  X,Y,Z= 0.89000E-01 0.11200          0.
NODE    22  KCS= 0  X,Y,Z= 0.57000E-01 0.45000E-01      0.
NODE    23  KCS= 0  X,Y,Z= 0.93000E-01 0.90000E-01      0.
NODE    24  KCS= 0  X,Y,Z= 0.97000E-01 0.90000E-01      0.
NODE    25  KCS= 0  X,Y,Z= 0.97000E-01 0.95000E-01      0.
NODE    26  KCS= 0  X,Y,Z= 0.97000E-01 0.10000          0.
NODE    27  KCS= 0  X,Y,Z= 0.93000E-01 0.10600          0.
NODE    28  KCS= 0  X,Y,Z= 0.11300     0.90000E-01      0.
NODE    29  KCS= 0  X,Y,Z= 0.12900     0.90000E-01      0.
NODE    30  KCS= 0  X,Y,Z= 0.12900     0.95000E-01      0.
NODE    31  KCS= 0  X,Y,Z= 0.12900     0.10000          0.
NODE    32  KCS= 0  X,Y,Z= 0.11300     0.10000          0.
NODE    33  KCS= 0  X,Y,Z= 0.16100     0.90000E-01      0.
NODE    34  KCS= 0  X,Y,Z= 0.19300     0.90000E-01      0.
NODE    35  KCS= 0  X,Y,Z= 0.19300     0.95000E-01      0.
NODE    36  KCS= 0  X,Y,Z= 0.16100     0.10000          0.
NODE    37  KCS= 0  X,Y,Z= 0.16100     0.56000E-01      0.
NODE    38  KCS= 0  X,Y,Z= 0.19300     0.22000E-01      0.
NODE    39  KCS= 0  X,Y,Z= 0.19300     0.56000E-01      0.
NODE    40  KCS= 0  X,Y,Z= 0.20550     0.90000E-01      0.
NODE    41  KCS= 0  X,Y,Z= 0.20550     0.10000          0.
NODE    42  KCS= 0  X,Y,Z= 0.21800     0.10000          0.
NODE    43  KCS= 0  X,Y,Z= 0.21800     0.95000E-01      0.
NODE    44  KCS= 0  X,Y,Z= 0.21800     0.90000E-01      0.
NODE    45  KCS= 0  X,Y,Z= 0.21800     0.56000E-01      0.
NODE    46  KCS= 0  X,Y,Z= 0.20550     0.22000E-01      0.
NODE    47  KCS= 0  X,Y,Z= 0.21800     0.22000E-01      0.
NODE    48  KCS= 0  X,Y,Z= 0.24650     0.56000E-01      0.
NODE    49  KCS= 0  X,Y,Z= 0.24650     0.90000E-01      0.
NODE    50  KCS= 0  X,Y,Z= 0.24650     0.10000          0.
```

```
NODE     51  KCS= 0  X,Y,Z= 0.27500     0.10000          0.
NODE     52  KCS= 0  X,Y,Z= 0.27500     0.95000E-01      0.
NODE     53  KCS= 0  X,Y,Z= 0.27500     0.90000E-01      0.
NODE     59  KCS= 0  X,Y,Z= 0.27900     0.10600          0.
NODE     60  KCS= 0  X,Y,Z= 0.28300     0.11200          0.
NODE     61  KCS= 0  X,Y,Z= 0.28300     0.10600          0.
NODE     62  KCS= 0  X,Y,Z= 0.28300     0.90000E-01      0.
NODE     63  KCS= 0  X,Y,Z= 0.27900     0.90000E-01      0.
NODE     64  KCS= 0  X,Y,Z= 0.29150     0.90000E-01      0.
NODE     65  KCS= 0  X,Y,Z= 0.30000     0.90000E-01      0.
NODE     66  KCS= 0  X,Y,Z= 0.30000     0.10100          0.
NODE     67  KCS= 0  X,Y,Z= 0.30000     0.11200          0.
NODE     68  KCS= 0  X,Y,Z= 0.29150     0.11200          0.
NODE     69  KCS= 0  X,Y,Z= 0.19300     0.10000          0.
NODE     74  KCS= 0  X,Y,Z= 0.30850     0.90000E-01      0.
NODE     75  KCS= 0  X,Y,Z= 0.30850     0.11200          0.
NODE     76  KCS= 0  X,Y,Z= 0.31700     0.11200          0.
NODE     77  KCS= 0  X,Y,Z= 0.31700     0.10100          0.
NODE     78  KCS= 0  X,Y,Z= 0.31700     0.90000E-01      0.
NODE     79  KCS= 0  X,Y,Z= 0.32100     0.90000E-01      0.
NODE     80  KCS= 0  X,Y,Z= 0.32500     0.90000E-01      0.
NODE     81  KCS= 0  X,Y,Z= 0.32500     0.95000E-01      0.
NODE     82  KCS= 0  X,Y,Z= 0.32500     0.10000          0.
NODE     83  KCS= 0  X,Y,Z= 0.32100     0.10600          0.
NODE     89  KCS= 0  X,Y,Z= 0.35350     0.10000          0.
NODE     90  KCS= 0  X,Y,Z= 0.38200     0.10000          0.
NODE     91  KCS= 0  X,Y,Z= 0.38200     0.95000E-01      0.
NODE     92  KCS= 0  X,Y,Z= 0.38200     0.90000E-01      0.
NODE     93  KCS= 0  X,Y,Z= 0.35350     0.90000E-01      0.
NODE     94  KCS= 0  X,Y,Z= 0.35350     0.56000E-01      0.
NODE     95  KCS= 0  X,Y,Z= 0.38200     0.22000E-01      0.
NODE     96  KCS= 0  X,Y,Z= 0.38200     0.56000E-01      0.
NODE     97  KCS= 0  X,Y,Z= 0.40700     0.22000E-01      0.
```

NODE 98 KCS= 0 X,Y,Z= 0.43900 0.56000E-01 0.

NODE 99 KCS= 0 X,Y,Z= 0.40700 0.56000E-01 0.

NODE 100 KCS= 0 X,Y,Z= 0.39450 0.90000E-01 0.

NODE 101 KCS= 0 X,Y,Z= 0.40700 0.90000E-01 0.

NODE 102 KCS= 0 X,Y,Z= 0.40700 0.95000E-01 0.

NODE 103 KCS= 0 X,Y,Z= 0.40700 0.10000 0.

NODE 104 KCS= 0 X,Y,Z= 0.39450 0.10000 0.

NODE 105 KCS= 0 X,Y,Z= 0.43900 0.10000 0.

NODE 106 KCS= 0 X,Y,Z= 0.50700 0.90000E-01 0.

NODE 107 KCS= 0 X,Y,Z= 0.47100 0.95000E-01 0.

NODE 108 KCS= 0 X,Y,Z= 0.43900 0.90000E-01 0.

NODE 109 KCS= 0 X,Y,Z= 0.47100 0.90000E-01 0.

NODE 110 KCS= 0 X,Y,Z= 0.47100 0.10000 0.

NODE 111 KCS= 0 X,Y,Z= 0.48700 0.10000 0.

NODE 112 KCS= 0 X,Y,Z= 0.50300 0.95000E-01 0.

NODE 113 KCS= 0 X,Y,Z= 0.48700 0.90000E-01 0.

NODE 114 KCS= 0 X,Y,Z= 0.50300 0.90000E-01 0.

NODE 115 KCS= 0 X,Y,Z= 0.51100 0.10100 0.

NODE 116 KCS= 0 X,Y,Z= 0.50700 0.10600 0.

NODE 117 KCS= 0 X,Y,Z= 0.51100 0.11200 0.

NODE 118 KCS= 0 X,Y,Z= 0.54300 0.11200 0.

NODE 119 KCS= 0 X,Y,Z= 0.57500 0.11200 0.

NODE 120 KCS= 0 X,Y,Z= 0.57500 0.10100 0.

NODE 121 KCS= 0 X,Y,Z= 0.57500 0.90000E-01 0.

NODE 122 KCS= 0 X,Y,Z= 0.54300 0.90000E-01 0.

NODE 123 KCS= 0 X,Y,Z= 0.54300 0.45000E-01 0.

NODE 124 KCS= 0 X,Y,Z= 0.57500 0. 0.

NODE 125 KCS= 0 X,Y,Z= 0.57500 0.45000E-01 0.

NODE 126 KCS= 0 X,Y,Z= 0.58750 0.90000E-01 0.

NODE 127 KCS= 0 X,Y,Z= 0.60000 0.90000E-01 0.

NODE 128 KCS= 0 X,Y,Z= 0.60000 0.10100 0.

NODE 129 KCS= 0 X,Y,Z= 0.60000 0.11200 0.

NODE 130 KCS= 0 X,Y,Z= 0.58750 0.11200 0.

NODE 131 KCS= 0 X,Y,Z= 0.60000 0.45000E-01 0.

NODE 132 KCS= 0 X,Y,Z= 0.51100 0.90000E-01 0.

NODE 133 KCS= 0 X,Y,Z= 0.50300 0.10000 0.

NODE 134 KCS= 0 X,Y,Z= 0.39450 0.22000E-01 0.

NODE 136 KCS= 0 X,Y,Z= 0.58750 0. 0.

NODE 135 KCS= 0 X,Y,Z= 0.60000 0. 0.

ELEMENT	1	1	11	13	3	6	12	8	2
ELEMENT	2	3	13	15	5	8	14	10	4
ELEMENT	3	13	19	21	15	16	20	18	14
ELEMENT	4	19	13	11	11	16	12	11	22
ELEMENT	5	19	24	26	21	23	25	27	20
ELEMENT	6	24	29	31	26	28	30	32	25
ELEMENT	7	29	34	69	31	33	35	36	30
ELEMENT	8	34	29	38	38	33	37	38	39
ELEMENT	9	38	47	44	34	46	45	40	39
ELEMENT	10	34	44	42	69	40	43	41	35
ELEMENT	11	44	53	51	42	49	52	50	43
ELEMENT	12	53	44	47	47	49	45	47	48

***WARNING *** CP= 5.710 TIME= 9.96222
ELEMENT 14. MIDSIDE NODE 61. MAY BE IMPROPERLY LOCATED
(MAY BE OK IF SINGULARITY IS DESIRED), RATIO= 0.227

ELEMENT	14	53	62	60	51	63	61	59	52
ELEMENT	15	62	65	67	60	64	66	68	71
ELEMENT	16	65	78	76	67	74	77	75	66
ELEMENT	17	78	80	82	76	79	81	83	77
ELEMENT	19	80	92	90	82	93	91	89	81
ELEMENT	20	92	80	95	95	93	94	95	96
ELEMENT	21	95	97	101	92	134	99	100	96
ELEMENT	22	109	101	97	97	108	99	97	98
ELEMENT	23	101	109	110	103	108	107	105	102
ELEMENT	24	92	101	103	90	100	102	104	91
ELEMENT	25	109	114	133	110	113	112	111	107
ELEMENT	26	114	132	117	133	106	115	116	112
ELEMENT	27	132	121	119	117	122	120	118	115
ELEMENT	28	121	132	124	124	122	123	124	125

```
 ELEMENT    29     127   121   124   135   126   125   136   131

 ELEMENT    30     121   127   129   119   126   128   130   120


 SPECIFIED DISP ALL  FOR SELECTED NODES IN RANGE     1 TO     1 BY    1
  VALUES=      0.          0.      ADDITIONAL DOFS=

 SPECIFIED DISP ALL  FOR SELECTED NODES IN RANGE     6 TO     6 BY    1
  VALUES=      0.          0.      ADDITIONAL DOFS=

 SPECIFIED DISP ALL  FOR SELECTED NODES IN RANGE    11 TO    11 BY    1
  VALUES=      0.          0.      ADDITIONAL DOFS=

 SPECIFIED DISP ALL  FOR SELECTED NODES IN RANGE   124 TO   124 BY    1
  VALUES=      0.          0.      ADDITIONAL DOFS=

 SPECIFIED DISP ALL  FOR SELECTED NODES IN RANGE   135 TO   135 BY    1
  VALUES=      0.          0.      ADDITIONAL DOFS=

 SPECIFIED DISP ALL  FOR SELECTED NODES IN RANGE   136 TO   136 BY    1
  VALUES=      0.          0.      ADDITIONAL DOFS=

 ELEMENT PRESSURE ON ELEM=     2  FACE=  3  PRESS=  1.30000000

 NUMBER OF ELEMENT PRESSURES=     1

 ELEMENT PRESSURE ON ELEM=     3  FACE=  3  PRESS=  1.30000000

 NUMBER OF ELEMENT PRESSURES=     2

 ELEMENT PRESSURE ON ELEM=     5  FACE=  3  PRESS=  1.30000000
 USE THIS SPECIFICATION FROM ELEMENT     5 TO     7  IN STEPS OF    1

 NUMBER OF ELEMENT PRESSURES=     5

 ELEMENT PRESSURE ON ELEM=    10  FACE=  3  PRESS=  1.30000000
 USE THIS SPECIFICATION FROM ELEMENT    10 TO    11  IN STEPS OF    1

 NUMBER OF ELEMENT PRESSURES=     7

 ELEMENT PRESSURE ON ELEM=    13  FACE=  3  PRESS=  1.30000000
 USE THIS SPECIFICATION FROM ELEMENT    13 TO    15  IN STEPS OF    1

 NUMBER OF ELEMENT PRESSURES=     9

 ***WARNING ***                                CP=      6.190   TIME=   9.96361
 SPECIFICATIONS REQUESTED FROM THE EP   COMMAND
 WHERE NOT STORED ON UNDEF OR UNSELECTED ELEMENTS.

 ELEMENT PRESSURE ON ELEM=    16  FACE=  3  PRESS=  1.30000000
 USE THIS SPECIFICATION FROM ELEMENT    16 TO    19  IN STEPS OF    1

 NUMBER OF ELEMENT PRESSURES=    12

 ***WARNING ***                                CP=      6.210   TIME=   9.96361
 SPECIFICATIONS REQUESTED FROM THE EP   COMMAND
 WHERE NOT STORED ON UNDEF OR UNSELECTED ELEMENTS.

 ELEMENT PRESSURE ON ELEM=    23  FACE=  3  PRESS=  1.30000000
 USE THIS SPECIFICATION FROM ELEMENT    23 TO    27  IN STEPS OF    1

 NUMBER OF ELEMENT PRESSURES=    17

 ELEMENT PRESSURE ON ELEM=    30  FACE=  3  PRESS=  1.30000000
```

```
 NUMBER OF ELEMENT PRESSURES=    18

 NITTER=      1  NPRINT=      1  NPOST=      1

 ALL PRINT CONTROLS RESET TO     1
  ALL POST DATA FILE CONTROLS RESET TO     1

 ALL  BOUNDARY CONDITION PLOT KEY =  1

 NODE NUMBERING KEY =  1

 ELEM NUMBERING KEY =  1

 ***WARNING ***                                CP=      6.670   TIME=    9.96417
 ELEMENT     14. MIDSIDE NODE     61. MAY BE IMPROPERLY LOCATED
  (MAY BE OK IF SINGULARITY IS DESIRED), RATIO=   0.227

 ***  NOTE  ***
 DATA CHECKED - NO FATAL ERRORS FOUND.
 CHECK OUTPUT FOR POSSIBLE WARNING MESSAGES.

 *** PREP7 GLOBAL STATUS ***

 TITLE= Beam Diaphragm structure,clearance=22u
 ANALYSIS TYPE=      0
 NUMBER OF ELEMENT TYPES=      1
     28 ELEMENTS CURRENTLY SELECTED.  MAX ELEMENT NUMBER =      30
    120 NODES CURRENTLY SELECTED.     MAX NODE NUMBER =       136
 MAXIMUM LINEAR PROPERTY NUMBER=      1
 ACTIVE COORDINATE SYSTEM=      0  (CARTESIAN)
 NUMBER OF IMPOSED DISPLACEMENTS=     12
 NUMBER OF ELEMENT PRESSURES=    18

 ANALYSIS DATA WRITTEN ON FILE27

 ALL CURRENT PREP7 DATA WRITTEN TO FILE16   NAME= file16.dat
  FOR POSSIBLE RESUME FROM THIS POINT


 ***** ROUTINE COMPLETED *****  CP =         7.800

 ***** INPUT SWITCHED FROM FILE18 TO FILE27  NAME=file27.dat

 NEW TITLE= Beam Diaphragm structure,clearance=22u

1            ANSYS - ENGINEERING ANALYSIS SYSTEM  REVISION 4.4      A 24   NEW JERS
      ANSYS(R)  COPYRIGHT(C) 1971, 1978, 1982, 1983, 1985, 1987, 1989, 1990   SWANS
      PROPRIETARY DATA - UNAUTHORIZED USE, DISTRIBUTION OR DUPLICATION IS PROHIBITE
      FOR SUPPORT CALL DAVID PEREL       PHONE (201) 596-3356    TWX

 Beam Diaphragm structure,clearance=22u
 **UNIVERSITY VERSION FOR EDUCATIONAL PURPOSES ONLY**


      *****  NOTICE  *****  THIS IS THE ANSYS GENERAL PURPOSE
      FINITE ELEMENT COMPUTER PROGRAM.  NEITHER SWANSON ANALYSIS
      SYSTEMS, INC. NOR THE DISTRIBUTOR SUPPLYING THIS PROGRAM
      ASSUME ANY RESPONSIBILITY FOR THE VALIDITY, ACCURACY, OR
      APPLICABILITY OF ANY RESULTS OBTAINED FROM THE ANSYS SYSTEM.
      USERS MUST VERIFY THEIR OWN RESULTS.

      ANSYS(R)  COPYRIGHT(C)  1971, 1978, 1982, 1983, 1985, 1987, 1989, 1990
      SWANSON ANALYSIS SYSTEMS, INC. AS AN UNPUBLISHED WORK.
      PROPRIETARY DATA - UNAUTHORIZED USE, DISTRIBUTION, OR DUPLICATION
      IS PROHIBITED.  ALL RIGHTS RESERVED.
```

SWANSON ANALYSIS SYSTEMS,INC. IS ENDEAVORING TO MAKE THE
ANSYS PROGRAM AS COMPLETE, ACCURATE, AND EASY TO USE AS
POSSIBLE. SUGGESTIONS AND COMMENTS ARE WELCOMED. ANY
ERRORS ENCOUNTERED IN EITHER THE DOCUMENTATION OR THE
RESULTS SHOULD BE IMMEDIATELY BROUGHT TO OUR ATTENTION.

***** ANALYSIS OPTIONS *****

	VALUE
ANALYSIS TYPE	0
REFERENCE TEMPERATURE	0.00

***** ELEMENT TYPES *****

TYPE	STIF	DESCRIPTION	KEY OPTIONS 1 2 3 4 5 6 7 8 9

NUMBER OF ELEMENT TYPES= 1

***** TABLE OF ELEMENT REAL CONSTANTS *****
NO.

NUMBER OF REAL CONSTANT SETS= 0

1 ANSYS - ENGINEERING ANALYSIS SYSTEM REVISION 4.4 A 24 NEW JERS
ANSYS(R) COPYRIGHT(C) 1971, 1978, 1982, 1983, 1985, 1987, 1989, 1990 SWANS
PROPRIETARY DATA - UNAUTHORIZED USE, DISTRIBUTION OR DUPLICATION IS PROHIBITI
FOR SUPPORT CALL DAVID PEREL PHONE (201) 596-3356 TWX

Beam Diaphragm structure,clearance=22u
UNIVERSITY VERSION FOR EDUCATIONAL PURPOSES ONLY

***** ELEMENT DEFINITIONS *****

ELEMENT	NODES	MAT	TYPE	ELEMENT

SWITCHED TO FIXED FORMAT INPUT

INTEGER STORAGE REQUIREMENTS FOR ELEMENT INPUT CP= 8.140 T
FIXED DATA = 1002 TEMPORARY DATA = 272 TOTAL= 1274
FIXED AVAIL= 1000000 TEMPORARY AVAIL= 1000000 TOTAL AVAIL= 1000000
MAXIMUM NODE NUMBER FOR AVAILABLE AUXILIARY MEMORY SIZE= 499498

NUMBER OF ELEMENTS = 30 MAXIMUM NODE NUMBER USED = 136

***** NODE DEFINITIONS *****

	LOCATION		ROTATION (DEGREES)
NODE	X (OR R)	Y (OR THETA)	THXY (OR RT)

```
 SWITCHED TO FIXED FORMAT INPUT

  XMIN=      0.       XMAX= 0.6000       YMIN=      0.       YMAX= 0.1120       ZMIN=

  INTEGER STORAGE REQUIREMENTS FOR NODE INPUT                          CP=      8.510  T
 FIXED DATA =     1002  TEMPORARY DATA =      816   TOTAL=     1818
 FIXED AVAIL= 1000000  TEMPORARY AVAIL= 1000000   TOTAL AVAIL= 1000000
  MAXIMUM NODE NUMBER FOR AVAILABLE AUXILIARY MEMORY SIZE=     332998


              ***** MATERIAL PROPERTIES *****

 MAXIMUM MATERIAL NUMBER=    1


              ***** MASTER DEGREES OF FREEDOM  *****

   NODE        DEGREES OF FREEDOM LIST


 NUMBER OF SPECIFIED MASTER D.O.F.=      0
 TOTAL NUMBER OF MASTER D.O.F.    =      0

  INTEGER STORAGE REQUIREMENTS FOR MATERIALS, ETC. INPUT               CP=      8.800  T
 FIXED DATA =       10  TEMPORARY DATA =        0   TOTAL=       10
 FIXED AVAIL= 1000000  TEMPORARY AVAIL= 1000000   TOTAL AVAIL= 1000000
1            ANSYS - ENGINEERING ANALYSIS SYSTEM  REVISION 4.4      A 24   NEW JERS
      ANSYS(R)  COPYRIGHT(C) 1971, 1978, 1982, 1983, 1985, 1987, 1989, 1990   SWANS
      PROPRIETARY DATA - UNAUTHORIZED USE, DISTRIBUTION OR DUPLICATION IS PROHIBITE
      FOR SUPPORT CALL DAVID PEREL       PHONE (201) 596-3356    TWX

 Beam Diaphragm structure,clearance=22u
 **UNIVERSITY VERSION FOR EDUCATIONAL PURPOSES ONLY**


 LOAD STEP NUMBER=     1

          *** LOAD OPTIONS SUMMARY ***

 TIME  =       0.      (TIME AT END OF LOAD STEP)
 NITTER=       1       (NUMBER OF ITERATIONS)
 TUNIF =    0.0000     (UNIFORM TEMPERATURE)    (TREF=    0.0000)
 KTEMP =    0          (USE TUNIF FOR ALL NODAL TEMPERATURES)
 KRF   =    2          (PRINT REACTION FORCES AT CONSTRAINED NODES)

 NPRINT=       1       (OVERALL PRINT FREQUENCY)
 NPOST =       1       (OVERALL POST FREQUENCY)

  DISPLACEMENT PRINT FREQUENCIES
   FREQ    NSTRT  NSTOP    NINC
      1        1 999999       1

  ELEMENT PRINT AND POST FREQUENCIES
   TYPE   STIFF  STRESS  FORCE       STRESS  STRESS  FORCE
          NO.    PRINT  PRINT       POST    LEVEL   POST
      1     82       1      1          1       3       1


 ***** LOAD SUMMARY -      12 DISPLACEMENTS        0 FORCES       18 PRESSURES      ***
```



```
  INTEGER STORAGE REQUIREMENTS FOR LOAD DATA INPUT                     CP=      9.200  T
```

```
 FIXED DATA =      378  TEMPORARY DATA =        0   TOTAL=      378
 FIXED AVAIL= 1000000  TEMPORARY AVAIL= 1000000   TOTAL AVAIL= 1000000

  RANGE OF ELEMENT MAXIMUM STIFFNESS IN GLOBAL COORDINATES


 MAXIMUM= 0.238065E+06  AT ELEMENT      23.
 MINIMUM= 0.387492E+05  AT ELEMENT      22.

  INTEGER STORAGE REQUIREMENTS FOR ELEMENT FORMULATION          CP=     10.930
 FIXED DATA =      378  TEMPORARY DATA =        0   TOTAL=      378
 FIXED AVAIL= 1000000  TEMPORARY AVAIL= 1000000   TOTAL AVAIL= 1000000

   *** ELEMENT STIFFNESS FORMULATION TIMES
  TYPE  NUMBER  STIF  TOTAL CP   AVE CP

    1      28    82     0.540    0.019


 TIME AT END OF ELEMENT STIFFNESS FORMULATION  CP=       10.940


 MAXIMUM IN-CORE WAVE FRONT ALLOWED FOR REQUESTED MEMORY SIZE=  500.

  INTEGER STORAGE REQUIREMENTS FOR WAVE FRONT MATRIX SOLUTION       CP=     11.830
 FIXED DATA =      378  TEMPORARY DATA =      676   TOTAL=     1054
 FIXED AVAIL= 1000000  TEMPORARY AVAIL= 1000000   TOTAL AVAIL= 1000000


 MAXIMUM IN-CORE WAVE FRONT=      24.


      MATRIX SOLUTION TIMES
  READ IN ELEMENT STIFFNESSES   CP=           0.220


  NODAL COORD. TRANSFORMATION   CP=           0.000
  MATRIX TRIANGULARIZATION      CP=           0.520


 TIME AT END OF MATRIX TRIANGULARIZATION  CP=          11.840
 EQUATION SOLVER MAXIMUM PIVOT= 0.11469E+06 AT NODE   101. UY
 EQUATION SOLVER MINIMUM PIVOT=  87.514     AT NODE    91. UY

  TIME AT START OF BACK SUBSTITUTION   CP=     11.910      LOAD STEP=   1  ITERATION
1            ANSYS - ENGINEERING ANALYSIS SYSTEM  REVISION 4.4      A 24   NEW JERS
      ANSYS(R)  COPYRIGHT(C) 1971, 1978, 1982, 1983, 1985, 1987, 1989, 1990   SWANS
      PROPRIETARY DATA - UNAUTHORIZED USE, DISTRIBUTION OR DUPLICATION IS PROHIBITE
      FOR SUPPORT CALL DAVID PEREL       PHONE (201) 596-3356    TWX

 Beam Diaphragm structure,clearance=22u
 **UNIVERSITY VERSION FOR EDUCATIONAL PURPOSES ONLY**


  ***** DISPLACEMENT SOLUTION *****  TIME =       0.      LOAD STEP=   1  ITERATION
    NODE      UX                UY

      1          0.                0.
      2    0.212233E-03      0.115102E-03
      3    0.640365E-03      0.156417E-03
      4    0.747853E-03      0.157858E-03
      5    0.853301E-03      0.157584E-03
      6          0.                0.
      8    0.638124E-03      0.388813E-04
     10    0.856275E-03      0.387927E-04
```

11	0.	0.
12	0.206882E-03	-0.790553E-04
13	0.638976E-03	-0.734292E-04
14	0.750647E-03	-0.795241E-04
15	0.863000E-03	-0.885402E-04
16	0.628196E-03	-0.402995E-03
18	0.903337E-03	-0.401383E-03
19	0.579397E-03	-0.854958E-03
20	0.808410E-03	-0.872718E-03
21	0.101852E-02	-0.895554E-03
22	0.201988E-03	-0.369259E-03
23	0.517993E-03	-0.973459E-03
24	0.398998E-03	-0.113297E-02
25	0.653553E-03	-0.109839E-02
26	0.846072E-03	-0.111455E-02
27	0.934052E-03	-0.978322E-03
28	-0.567152E-04	-0.265420E-02
29	-0.310328E-03	-0.528649E-02
30	0.596509E-03	-0.527629E-02
31	0.151453E-02	-0.527334E-02
32	0.128009E-02	-0.265180E-02
33	-0.344910E-03	-0.112548E-01
34	-0.367508E-03	-0.171775E-01
35	0.543187E-03	-0.171715E-01
36	0.152263E-02	-0.112580E-01
37	-0.662682E-02	-0.112666E-01
38	-0.128346E-01	-0.171564E-01
39	-0.662005E-02	-0.171660E-01
40	-0.388833E-03	-0.194672E-01
41	0.142674E-02	-0.194659E-01
42	0.137717E-02	-0.217001E-01
43	0.473989E-03	-0.217239E-01
44	-0.407965E-03	-0.217488E-01
45	-0.659250E-02	-0.217514E-01
46	-0.128516E-01	-0.194474E-01
47	-0.128702E-01	-0.217503E-01
48	-0.657196E-02	-0.269272E-01
49	-0.458171E-03	-0.269325E-01
50	0.136105E-02	-0.269608E-01
51	0.981760E-03	-0.317940E-01
52	0.317071E-03	-0.318376E-01
53	-0.399472E-03	-0.318719E-01
59	0.103081E-02	-0.326735E-01

1 ANSYS - ENGINEERING ANALYSIS SYSTEM REVISION 4.4 A 24 NEW JERS
ANSYS(R) COPYRIGHT(C) 1971, 1978, 1982, 1983, 1985, 1987, 1989, 1990 SWANS
PROPRIETARY DATA - UNAUTHORIZED USE, DISTRIBUTION OR DUPLICATION IS PROHIBITE
FOR SUPPORT CALL DAVID PEREL PHONE (201) 596-3356 TWX

Beam Diaphragm structure,clearance=22u
UNIVERSITY VERSION FOR EDUCATIONAL PURPOSES ONLY

***** DISPLACEMENT SOLUTION ***** TIME = 0. LOAD STEP= 1 ITERATION

NODE	UX	UY
60	-0.109638E-02	-0.321846E-01
61	0.742090E-03	-0.323381E-01
62	0.999384E-04	-0.328605E-01
63	-0.293084E-03	-0.323505E-01
64	-0.326863E-04	-0.319607E-01
65	-0.126077E-03	-0.314832E-01
66	-0.736069E-03	-0.314897E-01
67	-0.164977E-02	-0.314589E-01
68	-0.139122E-02	-0.320967E-01
69	0.144963E-02	-0.171616E-01

71	-0.907132E-03	-0.325372E-01
74	0.445776E-04	-0.309038E-01
75	-0.164210E-02	-0.308062E-01
76	-0.162950E-02	-0.301760E-01
77	-0.864740E-03	-0.301816E-01
78	0.212898E-03	-0.301778E-01
79	0.270835E-03	-0.297856E-01
80	0.373842E-03	-0.294026E-01
81	-0.272250E-03	-0.293805E-01
82	-0.866447E-03	-0.293467E-01
83	-0.128630E-02	-0.298359E-01
89	-0.123897E-02	-0.249103E-01
90	-0.125763E-02	-0.200889E-01
91	-0.428119E-03	-0.201065E-01
92	0.380430E-03	-0.201261E-01
93	0.431926E-03	-0.248898E-01
94	0.604161E-02	-0.248844E-01
95	0.118395E-01	-0.201290E-01
96	0.606245E-02	-0.201297E-01
97	0.118024E-01	-0.159044E-01
98	0.609847E-02	-0.104857E-01
99	0.609105E-02	-0.159136E-01
100	0.361221E-03	-0.180314E-01
101	0.339327E-03	-0.159248E-01
102	-0.498282E-03	-0.159196E-01
103	-0.133194E-02	-0.159106E-01
104	-0.130734E-02	-0.180280E-01
105	-0.140389E-02	-0.104771E-01
106	-0.483695E-03	-0.924884E-03
107	-0.556014E-03	-0.496039E-02
108	0.315706E-03	-0.104743E-01
109	0.283506E-03	-0.497009E-02
110	-0.140621E-02	-0.495694E-02
111	-0.119877E-02	-0.251062E-02
112	-0.612281E-03	-0.104424E-02
113	0.556548E-04	-0.251294E-02
114	-0.370827E-03	-0.107688E-02
115	-0.759823E-03	-0.828709E-03
116	-0.879223E-03	-0.929172E-03
117	-0.959732E-03	-0.850502E-03
118	-0.849990E-03	-0.380756E-03

1 ANSYS - ENGINEERING ANALYSIS SYSTEM REVISION 4.4 A 24 NEW JERS
ANSYS(R) COPYRIGHT(C) 1971, 1978, 1982, 1983, 1985, 1987, 1989, 1990 SWANS
PROPRIETARY DATA - UNAUTHORIZED USE, DISTRIBUTION OR DUPLICATION IS PROHIBITE
FOR SUPPORT CALL DAVID PEREL PHONE (201) 596-3356 TWX

Beam Diaphragm structure,clearance=22u
UNIVERSITY VERSION FOR EDUCATIONAL PURPOSES ONLY

***** DISPLACEMENT SOLUTION ***** TIME = 0. LOAD STEP= 1 ITERATION

NODE	UX	UY
119	-0.811325E-03	-0.848175E-04
120	-0.705130E-03	-0.762146E-04
121	-0.599497E-03	-0.703996E-04
122	-0.589163E-03	-0.382214E-03
123	-0.187284E-03	-0.349554E-03
124	0.	0.
125	-0.192217E-03	-0.753354E-04
126	-0.598711E-03	0.357645E-04
127	-0.600835E-03	0.146756E-03
128	-0.702401E-03	0.148132E-03
129	-0.802129E-03	0.147887E-03
130	-0.804930E-03	0.355501E-04

```
131   -0.197329E-03    0.107267E-03
132   -0.542262E-03   -0.811763E-03
133   -0.794953E-03   -0.105905E-02
134    0.118200E-01   -0.180096E-01
135          0.              0.
136          0.              0.

MAXIMUMS
NODE         47              62
VALUE   -0.128702E-01   -0.328605E-01

 INTEGER STORAGE REQUIREMENTS FOR BACK SUBSTITUTION                CP=     12.380
FIXED DATA =      378  TEMPORARY DATA =      550   TOTAL=      928
FIXED AVAIL= 1000000  TEMPORARY AVAIL= 1000000   TOTAL AVAIL= 1000000
1            ANSYS - ENGINEERING ANALYSIS SYSTEM  REVISION 4.4      A 24   NEW JER
     ANSYS(R)  COPYRIGHT(C) 1971, 1978, 1982, 1983, 1985, 1987, 1989, 1990   SWAN
     PROPRIETARY DATA - UNAUTHORIZED USE, DISTRIBUTION OR DUPLICATION IS PROHIBIT
     FOR SUPPORT CALL DAVID PEREL       PHONE (201) 596-3356    TWX

Beam Diaphragm structure,clearance=22u
**UNIVERSITY VERSION FOR EDUCATIONAL PURPOSES ONLY**

  ***** ELEMENT STRESSES *****  TIME =        0.       LOAD STEP=    1   ITERATIO

EL=     1  NODES=     1    11    13     3     6    12     8     2   MAT=  1   VOL
XC,YC= 0.1250E-01 0.4500E-01  TEMP=   0.0  SX,SY,SXY,SZ= -0.40628       8.2702
 SIG1,SIG2,SIG3=     9.1073              0.        -1.2434     S.I.=     10.351

EL=     2  NODES=     3    13    15     5     8    14    10     4   MAT=  1   VOL
XC,YC= 0.1250E-01 0.1010      TEMP=   0.0  SX,SY,SXY,SZ=   2.0343      -1.4478
 SIG1,SIG2,SIG3=     3.8068              0.        -3.2203     S.I.=     7.0270

EL=     3  NODES=    13    19    21    15    16    20    18    14   MAT=  1   VOL
XC,YC= 0.5700E-01 0.1010      TEMP=   0.0  SX,SY,SXY,SZ=   15.442      -2.4579
 SIG1,SIG2,SIG3=     17.873              0.        -4.8894     S.I.=     22.763

EL=     4  NODES=    19    13    11    11    16    12    11    22   MAT=  1   VOL
XC,YC= 0.4633E-01 0.6000E-01  TEMP=   0.0  SX,SY,SXY,SZ=  -13.442      -18.696
 SIG1,SIG2,SIG3=          0.       -5.2539        -26.884     S.I.=     26.884

EL=     5  NODES=    19    24    26    21    23    25    27    20   MAT=  1   VOL
XC,YC= 0.9300E-01 0.9800E-01  TEMP=   0.0  SX,SY,SXY,SZ=  -16.812      -9.0904
 SIG1,SIG2,SIG3=     5.1672              0.        -31.070     S.I.=     36.237

EL=     6  NODES=    24    29    31    26    28    30    32    25   MAT=  1   VOL
XC,YC= 0.1130      0.9500E-01  TEMP=   0.0  SX,SY,SXY,SZ=  -24.956       5.5604
 SIG1,SIG2,SIG3=     19.132              0.        -38.528     S.I.=     57.660

EL=     7  NODES=    29    34    69    31    33    35    36    30   MAT=  1   VOL
XC,YC= 0.1610      0.9500E-01  TEMP=   0.0  SX,SY,SXY,SZ=  -16.550      0.14621
 SIG1,SIG2,SIG3=     1.3328              0.        -17.737     S.I.=     19.069

EL=     8  NODES=    34    29    38    38    33    37    38    39   MAT=  1   VOL
XC,YC= 0.1717      0.6733E-01  TEMP=   0.0  SX,SY,SXY,SZ=  -2.4724       1.6974
 SIG1,SIG2,SIG3=     4.1270              0.        -4.9021     S.I.=     9.0291

EL=     9  NODES=    38    47    44    34    46    45    40    39   MAT=  1   VOL
XC,YC= 0.2055      0.5600E-01  TEMP=   0.0  SX,SY,SXY,SZ=   3.2336      -3.6402
 SIG1,SIG2,SIG3=     3.3032              0.        -3.7098     S.I.=     7.0131

EL=    10  NODES=    34    44    42    69    40    43    41    35   MAT=  1   VOL
XC,YC= 0.2055      0.9500E-01  TEMP=   0.0  SX,SY,SXY,SZ=  -46.944       8.0613
 SIG1,SIG2,SIG3=     9.1208              0.        -48.004     S.I.=     57.125

EL=    11  NODES=    44    53    51    42    49    52    50    43   MAT=  1   VOL
XC,YC= 0.2465      0.9500E-01  TEMP=   0.0  SX,SY,SXY,SZ=  -60.516      -13.833
```

```
 SIG1,SIG2,SIG3=          0.        -3.3596        -70.989     S.I.=      70.989

EL=     12  NODES=     53     44     47     47     49     45     47     48   MAT=  1   VOL=
XC,YC= 0.2370      0.6733E-01  TEMP=    0.0  SX,SY,SXY,SZ=    10.459        1.2873
 SIG1,SIG2,SIG3=      12.736              0.        -0.98998     S.I.=      13.726

EL=     14  NODES=     53     62     60     51     63     61     59     52   MAT=  1   VOL=
XC,YC= 0.2790      0.1005      TEMP=    0.0  SX,SY,SXY,SZ=   -88.642       -291.38
 SIG1,SIG2,SIG3=          0.        -48.316        -331.71     S.I.=      331.71

EL=     15  NODES=     62     65     67     60     64     66     68     71   MAT=  1   VOL=
XC,YC= 0.2915      0.1010      TEMP=    0.0  SX,SY,SXY,SZ=   -12.053        18.907
 SIG1,SIG2,SIG3=      18.917              0.        -12.063     S.I.=      30.981

EL=     16  NODES=     65     78     76     67     74     77     75     66   MAT=  1   VOL=
XC,YC= 0.3085      0.1010      TEMP=    0.0  SX,SY,SXY,SZ=   -12.053        56.339
 SIG1,SIG2,SIG3=      56.341              0.        -12.056     S.I.=      68.397

EL=     17  NODES=     78     80     82     76     79     81     83     77   MAT=  1   VOL=
XC,YC= 0.3210      0.9800E-01  TEMP=    0.0  SX,SY,SXY,SZ=   -16.812       -30.601
 SIG1,SIG2,SIG3=          0.        -16.598        -30.816     S.I.=      30.816

EL=     19  NODES=     80     92     90     82     93     91     89     81   MAT=  1   VOL=
XC,YC= 0.3535      0.9500E-01  TEMP=    0.0  SX,SY,SXY,SZ=   -60.386       -14.606
 SIG1,SIG2,SIG3=          0.        -4.2640        -70.728     S.I.=      70.728

EL=     20  NODES=     92     80     95     95     93     94     95     96   MAT=  1   VOL=
XC,YC= 0.3630      0.6733E-01  TEMP=    0.0  SX,SY,SXY,SZ=    10.420        1.4130
 SIG1,SIG2,SIG3=      12.709              0.        -0.87569     S.I.=      13.585

EL=     21  NODES=     95     97    101     92    134     99    100     96   MAT=  1   VOL=
XC,YC= 0.3945      0.5600E-01  TEMP=    0.0  SX,SY,SXY,SZ=    3.4428       -3.8251
 SIG1,SIG2,SIG3=      3.4888              0.        -3.8710     S.I.=      7.3598

EL=     22  NODES=    109    101     97     97    108     99     97     98   MAT=  1   VOL=
XC,YC= 0.4283      0.6733E-01  TEMP=    0.0  SX,SY,SXY,SZ=   -2.0676        1.7299
 SIG1,SIG2,SIG3=      4.3272              0.        -4.6649     S.I.=      8.9921

EL=     23  NODES=    101    109    110    103    108    107    105    102   MAT=  1   VOL=
XC,YC= 0.4390      0.9500E-01  TEMP=    0.0  SX,SY,SXY,SZ=   -17.926      -0.21005
 SIG1,SIG2,SIG3=     0.67710              0.        -18.813     S.I.=      19.490

EL=     24  NODES=     92    101    103     90    100    102    104     91   MAT=  1   VOL=
XC,YC= 0.3945      0.9500E-01  TEMP=    0.0  SX,SY,SXY,SZ=   -48.367        6.0016
 SIG1,SIG2,SIG3=      7.2086              0.        -49.574     S.I.=      56.783

EL=     25  NODES=    109    114    133    110    113    112    111    107   MAT=  1   VOL=
XC,YC= 0.4870      0.9500E-01  TEMP=    0.0  SX,SY,SXY,SZ=   -24.956        5.2637
 SIG1,SIG2,SIG3=      18.649              0.        -38.341     S.I.=      56.990

EL=     26  NODES=    114    132    117    133    106    115    116    112   MAT=  1   VOL=
XC,YC= 0.5070      0.9800E-01  TEMP=    0.0  SX,SY,SXY,SZ=   -16.812       -8.5414
 SIG1,SIG2,SIG3=      5.3093              0.        -30.663     S.I.=      35.972

EL=     27  NODES=    132    121    119    117    122    120    118    115   MAT=  1   VOL=
XC,YC= 0.5430      0.1010      TEMP=    0.0  SX,SY,SXY,SZ=    14.607       -2.4296
 SIG1,SIG2,SIG3=      16.887              0.        -4.7098     S.I.=      21.597

EL=     28  NODES=    121    132    124    124    122    123    124    125   MAT=  1   VOL=
XC,YC= 0.5537      0.6000E-01  TEMP=    0.0  SX,SY,SXY,SZ=   -13.034       -18.057
 SIG1,SIG2,SIG3=          0.        -5.0107        -26.080     S.I.=      26.080

EL=     29  NODES=    127    121    124    135    126    125    136    131   MAT=  1   VOL=
XC,YC= 0.5875      0.4500E-01  TEMP=    0.0  SX,SY,SXY,SZ= -0.48734        7.5739
 SIG1,SIG2,SIG3=      8.2806              0.        -1.1940     S.I.=      9.4746
```

```
 EL=    30  NODES=   121   127   129   119   126   128   130   120   MAT=  1   VOL=
 XC,YC= 0.5875     0.1010      TEMP=   0.0  SX,SY,SXY,SZ=   1.9423      -1.4533
  SIG1,SIG2,SIG3=     3.6068            0.       -3.1178     S.I.=     6.7246
1            ANSYS - ENGINEERING ANALYSIS SYSTEM  REVISION 4.4      A 24   NEW JER
      ANSYS(R)  COPYRIGHT(C) 1971, 1978, 1982, 1983, 1985, 1987, 1989, 1990   SWAN
      PROPRIETARY DATA - UNAUTHORIZED USE, DISTRIBUTION OR DUPLICATION IS PROHIBIT
      FOR SUPPORT CALL DAVID PEREL       PHONE (201) 596-3356    TWX

 Beam Diaphragm structure,clearance=22u
 **UNIVERSITY VERSION FOR EDUCATIONAL PURPOSES ONLY**

   ***** REACTION FORCES *****   TIME =       0.      LOAD STEP=    1  ITERATION=

  NOTE - REACTION FORCES ARE IN THE NODAL COORDINATE SYSTEM.


    NODE      FX              FY

      1   -0.283249       -0.214660
      6    0.550118       -0.180419
     11   -0.170854E-02    0.786590
    124   -0.363814E-02    0.742606
    135    0.259262       -0.189134
    136   -0.520784       -0.164983

 TOTAL   -0.656919E-12    0.780000

   *** ELEM. STRESS CALC. TIMES
  TYPE  NUMBER  STIF  TOTAL CP   AVE CP

   1      28     82     0.840   0.030

   *** NODAL FORCE CALC. TIMES
  TYPE  NUMBER  STIF  TOTAL CP   AVE CP

   1      28     82     0.110   0.004

 *** LOAD STEP    1   ITER     1  COMPLETED.  TIME=        0.      TIME INC=

  INTEGER STORAGE REQUIREMENTS FOR STRESS AND FORCE CALCULATIONS   CP=    14.070  T
 FIXED DATA =      378  TEMPORARY DATA =    1632   TOTAL=    2010
 FIXED AVAIL= 1000000  TEMPORARY AVAIL= 1000000   TOTAL AVAIL= 1000000


  *** STORAGE REQUIREMENT SUMMARY
 MAXIMUM FIXED MEMORY USED    =       1002
 MAXIMUM TEMPORARY MEMORY USED=       1632
 MAXIMUM TOTAL MEMORY USED    =       2010
 MAXIMUM TEMPORARY AVAILABLE  =     999620


   *** PROBLEM STATISTICS
  NO. OF ACTIVE DEGREES OF FREEDOM =    228
  R.M.S. WAVEFRONT SIZE =    14.4


  *** ANSYS BINARY FILE STATISTICS
 BUFFER SIZE USED= 2048
 POST DATA WRITTEN ON FILE12
 RESTART DATA WRITTEN ON FILE03   (          89540 BYTES)
 TRIANGULARIZED MATRIX WRITTEN ON FILE11   (          31708 BYTES)

 ***** END OF INPUT ENCOUNTERED ON FILE27.  FILE27 REWOUND

 ***** INPUT FILE SWITCHED FROM FILE27 TO FILE18
```

```
1           ANSYS - ENGINEERING ANALYSIS SYSTEM  REVISION 4.4      A 24   NEW JERS
      ANSYS(R)  COPYRIGHT(C) 1971, 1978, 1982, 1983, 1985, 1987, 1989, 1990   SWANS
      PROPRIETARY DATA - UNAUTHORIZED USE, DISTRIBUTION OR DUPLICATION IS PROHIBITE
      FOR SUPPORT CALL DAVID PEREL       PHONE (201) 596-3356    TWX

 Beam Diaphragm structure,clearance=22u
 **UNIVERSITY VERSION FOR EDUCATIONAL PURPOSES ONLY**


 ***** ANSYS SOLUTION PHASE RUN TIME ESTIMATOR *****

 COMPUTER = SUN4                      NUMBER OF MASTER DOF =    0
 ANALYSIS TYPE =  0                   RMS WAVE FRONT =   15
 NUMBER OF ACTIVE NODES =     115     TOTAL NO. OF ITERATIONS =     1
 MAX. DOF PER NODE =  2               STIFF. MATRIX SAVE KEY = 0
 NUMBER OF MATRICES = 1               ELEM. MATRIX SAVE KEY = 0
 NUMBER OF STRESS SOLUTIONS=    1     ROTATED NODE FRACTION= 0.000

   STIF  NUMBER    FORM. TIME  STRESS TIME    NAME
    82      28         0.027        0.018   MULTI-NODE STRESS SOLID, 2-D


                          FIRST     SUBSEQUENT
   ANALYSIS PHASE       ITERATION   ITERATIONS      TOTAL

 ELEMENT FORMULATION        0.90        0.90        0.90
 NODE ROTATION              0.00        0.00        0.00
 WAVE FRONT SOLUTION        0.07        0.07        0.07
 BACK SUBSTITUTION          0.02        0.02        0.02
 ELEMENT STRESSES           0.61        0.61        0.61
 NODAL FORCES               0.03        0.03        0.03

     TOTAL TIME (SEC)       1.64        1.64        1.64


 ***** ROUTINE COMPLETED *****  CP =         14.160
1           ANSYS - ENGINEERING ANALYSIS SYSTEM  REVISION 4.4      A 24   NEW JERS
      ANSYS(R)  COPYRIGHT(C) 1971, 1978, 1982, 1983, 1985, 1987, 1989, 1990   SWANS
      PROPRIETARY DATA - UNAUTHORIZED USE, DISTRIBUTION OR DUPLICATION IS PROHIBITE
      FOR SUPPORT CALL DAVID PEREL       PHONE (201) 596-3356    TWX

 Beam Diaphragm structure,clearance=22u
 **UNIVERSITY VERSION FOR EDUCATIONAL PURPOSES ONLY**

          ***** ANSYS RESULTS INTERPRETATION (POST1) *****

 USE LOAD STEP     1  ITERATION     1  SECTION   1  FOR LOAD CASE     1


 GEOMETRY STORED FOR    120  NODES     28  ELEMENTS
  TITLE= Beam Diaphragm structure,clearance=22u

 DISPLACEMENT STORED FOR  120 NODES

 STRESSES STORED FOR    4  SELECTED ITEMS

 NODAL STRESSES AND TEMPS. STORED FOR   28 ELEMENTS

 ITERATION SUMMARY INFORMATION STORED

 NODAL FORCES STORED FOR   28 ELEMENTS

 REACTIONS STORED FOR   12 REACTIONS
```

FOR LOAD STEP= 1 ITERATION= 1 SECTION= 1
TIME= 0. LOAD CASE= 1
TITLE= Beam Diaphragm structure,clearance=22u

USE GLOBAL COORDINATES FOR DISPLACEMENTS, FORCES, AND COMPONENT STRESSES

PRINT COMPONENT NODAL STRESSES PER ELEMENT

1 ANSYS - ENGINEERING ANALYSIS SYSTEM REVISION 4.4 A 24 NEW JER
ANSYS(R) COPYRIGHT(C) 1971, 1978, 1982, 1983, 1985, 1987, 1989, 1990 SWAN
PROPRIETARY DATA - UNAUTHORIZED USE, DISTRIBUTION OR DUPLICATION IS PROHIBIT
FOR SUPPORT CALL DAVID PEREL PHONE (201) 596-3356 TWX

Beam Diaphragm structure,clearance=22u
UNIVERSITY VERSION FOR EDUCATIONAL PURPOSES ONLY

***** POST1 ELEMENT NODAL STRESS LISTING *****

LOAD STEP 1 ITERATION= 1 SECTION= 1
TIME= 0. LOAD CASE= 1

THE FOLLOWING X,Y,Z STRESSES ARE IN GLOBAL COORDINATES

NODE	SX	SY	SZ	SXY	SYZ
ELEMENT= 1		STIF 82			
1	18.442655	69.340812	0.	1.4108731	
11	-19.611775	-57.507288	0.	-0.21445362	
13	7.9688543	22.275641	0.	8.8001854	
3	-8.4248565	-1.0282272	0.	1.2913858	
6	-0.58456041	5.9167618	0.	0.59820973	
12	-5.8214606	-17.615824	0.	4.2928659	
8	-0.22800112	10.623707	0.	5.0457856	
2	5.0088991	34.156292	0.	1.3511294	
ELEMENT= 2		STIF 82			
3	-4.4676740	6.5948751	0.	1.8898220	
13	1.9163708	-3.4668101	0.	9.8742714	
15	8.9502044	-11.447964	0.	-2.0264827	
5	1.7383337	2.5286770	0.	2.4696239	
8	-1.2756516	1.5640325	0.	5.8820467	
14	5.4332876	-7.4573868	0.	3.9238944	
10	5.3442691	-4.4596433	0.	0.22157059	
4	-1.3646701	4.5617761	0.	2.1797229	
ELEMENT= 3		STIF 82			
13	10.453437	12.096515	0.	0.26078633	
19	-45.188053	-22.885264	0.	28.818795	
21	92.841746	0.99029958	0.	-12.669753	
15	3.6593571	-0.33012508E-01	0.	11.714258	
16	-17.367308	-5.3943742	0.	14.539791	
20	23.826847	-10.947482	0.	8.0745212	
18	48.250552	0.47864353	0.	-0.47774730	
14	7.0563972	6.0317513	0.	5.9875222	
ELEMENT= 4		STIF 82			
19	-48.524001	-27.543764	0.	-30.644326	
13	12.046024	23.866464	0.	27.169657	
11	-3.8471380	-52.410225	0.	-27.998236	
11	-3.8471380	-52.410225	0.	-27.998236	
16	-18.238988	-1.8386504	0.	-1.7373343	
12	4.0994432	-14.271881	0.	-0.41428916	
11	-3.8471380	-52.410225	0.	-27.998236	
22	-26.185569	-39.976995	0.	-29.321281	
ELEMENT= 5		STIF 82			
19	-138.36240	-85.404667	0.	-34.541050	

24	-562.16199	20.483719	0.	74.525924
26	516.90344	24.900005	0.	-122.55743
21	116.37215	3.6593152	0.	11.763093
23	-350.26219	-32.460474	0.	19.992437
25	-22.629274	22.691862	0.	-24.015754
27	316.63779	14.279660	0.	-55.397169
20	-10.995124	-40.872676	0.	-11.388979

1 ANSYS - ENGINEERING ANALYSIS SYSTEM REVISION 4.4 A 24 NEW JERS

ANSYS(R) COPYRIGHT(C) 1971, 1978, 1982, 1983, 1985, 1987, 1989, 1990 SWANS
PROPRIETARY DATA - UNAUTHORIZED USE, DISTRIBUTION OR DUPLICATION IS PROHIBITI
FOR SUPPORT CALL DAVID PEREL PHONE (201) 596-3356 TWX

Beam Diaphragm structure,clearance=22u
UNIVERSITY VERSION FOR EDUCATIONAL PURPOSES ONLY

***** POST1 ELEMENT NODAL STRESS LISTING *****

LOAD STEP 1 ITERATION= 1 SECTION= 1
TIME= 0. LOAD CASE= 1

THE FOLLOWING X,Y,Z STRESSES ARE IN GLOBAL COORDINATES

NODE	SX	SY	SZ	SXY	SYZ
ELEMENT= 6		STIF 82			
24	-672.94149	9.0204346	0.	70.841282	
29	-203.28821	-25.429220	0.	-44.238893	
31	153.37600	26.531554	0.	-0.52332414	
26	623.02929	12.118935	0.	-123.92350	
28	-438.11485	-8.2043929	0.	13.301194	
30	-24.956104	0.55116672	0.	-22.381109	
32	388.20264	19.325244	0.	-62.223411	
25	-24.956104	10.569685	0.	-26.541109	
ELEMENT= 7		STIF 82			
29	-14.897311	25.552156	0.	-28.720222	
34	-11.544194	-10.705311	0.	9.0631891	
69	-64.939877	3.2006857	0.	5.0532509	
31	25.181453	-17.462703	0.	-3.8222118	
33	-13.220753	7.4234222	0.	-9.8285166	
35	-38.242036	-3.7523128	0.	7.0582200	
36	-19.879212	-7.1310089	0.	0.61551952	
30	5.1420710	4.0447262	0.	-16.271217	
ELEMENT= 8		STIF 82			
34	-13.114774	-10.848199	0.	0.64271763	
29	-20.177197	13.044914	0.	-7.5983509	
38	25.874806	2.8954046	0.	-5.0572579	
38	25.874806	2.8954046	0.	-5.0572579	
33	-16.645986	1.0983574	0.	-3.4778167	
37	2.8488041	7.9701593	0.	-6.3278044	
38	25.874806	2.8954046	0.	-5.0572579	
39	6.3800157	-3.9763972	0.	-2.2072701	
ELEMENT= 9		STIF 82			
38	7.3131752	-4.5447031	0.	-4.8817545	
47	2.8683365	-2.6706992	0.	8.7553401	
44	6.5882540	2.5907105	0.	-12.949857	
34	-3.8354753	-9.9360280	0.	6.2945236	
46	5.0907558	-3.6077012	0.	1.9367928	
45	4.7282953	-0.39994332E-01	0.	-2.0972584	
40	1.3763893	-3.6726587	0.	-3.3276666	
39	1.7388499	-7.2403656	0.	0.70638455	
ELEMENT= 10		STIF 82			
34	-52.457917	-39.743528	0.	0.67063965	

44	-18.163767	52.351281	0.	-50.489364	
42	-96.053256	20.049584	0.	57.389861	
69	-21.102649	-0.41224572	0.	-38.399687	
40	-35.310842	6.3038763	0.	-24.909362	
43	-57.108511	36.200432	0.	3.4502484	
41	-58.577952	9.8186693	0.	9.4950872	
35	-36.780283	-20.077887	0.	-18.864524	

1 ANSYS - ENGINEERING ANALYSIS SYSTEM REVISION 4.4 A 24 NEW JERS
ANSYS(R) COPYRIGHT(C) 1971, 1978, 1982, 1983, 1985, 1987, 1989, 1990 SWANS
PROPRIETARY DATA - UNAUTHORIZED USE, DISTRIBUTION OR DUPLICATION IS PROHIBITI
FOR SUPPORT CALL DAVID PEREL PHONE (201) 596-3356 TWX

Beam Diaphragm structure,clearance=22u
UNIVERSITY VERSION FOR EDUCATIONAL PURPOSES ONLY

***** POST1 ELEMENT NODAL STRESS LISTING *****

LOAD STEP 1 ITERATION= 1 SECTION= 1
TIME= 0. LOAD CASE= 1

THE FOLLOWING X,Y,Z STRESSES ARE IN GLOBAL COORDINATES

NODE	SX	SY	SZ	SXY	SYZ
ELEMENT= 11		STIF 82			
44	-73.984343	-41.106076	0.	27.576226	
53	90.710744	23.852600	0.	-35.486474	
51	-379.75978	-46.524307	0.	-136.37081	
42	120.97001	8.4453812	0.	46.413862	
49	8.3632006	-8.6267379	0.	-3.9551241	
52	-144.52452	-11.335853	0.	-85.928640	
50	-129.39488	-19.039463	0.	-44.978472	
43	23.492835	-16.330347	0.	36.995044	
ELEMENT= 12		STIF 82			
53	80.793108	17.860743	0.	53.651692	
44	-75.853674	-20.270249	0.	-41.223911	
47	26.436805	6.2714600	0.	2.8904749	
47	26.436805	6.2714600	0.	2.8904749	
49	2.4697170	-1.2047533	0.	6.2138904	
45	-24.708434	-6.9993946	0.	-19.166718	
47	26.436805	6.2714600	0.	2.8904749	
48	53.614957	12.066101	0.	28.271084	
ELEMENT= 14		STIF 82			
53	635.79756	-113.84173	0.	496.66900	
62	71.899618	796.36834	0.	329.17733	
60	-250.93453	-778.87034	0.	-657.93107	
51	-811.33161	-1069.1769	0.	-563.93495	
63	353.84859	341.26331	0.	412.92317	
61	-89.517459	8.7489991	0.	-164.37687	
59	-531.13307	-924.02364	0.	-610.93301	
52	-87.767025	-591.50933	0.	-33.632973	
ELEMENT= 15		STIF 82			
62	168.69492	303.91613	0.	13.553474	
65	171.34209	-271.93080	0.	-76.115221	
67	-195.44764	-253.04965	0.	75.977850	
60	-192.80047	296.69221	0.	-15.699937	
64	170.01851	15.992664	0.	-31.280873	
66	-12.052774	-262.49022	0.	-0.68685700E-01	
68	-194.12406	21.821284	0.	30.138956	
71	-12.052774	300.30417	0.	-1.0732312	
ELEMENT= 16		STIF 82			
65	171.34209	56.605535	0.	133.82689	

78	169.33183	84.681652	0.	-129.38893
76	-193.43738	8.5809452	0.	131.26065
67	-195.44764	75.486691	0.	-133.96426
74	170.33696	70.643593	0.	2.2189816
77	-12.052774	46.631299	0.	0.93585975
75	-194.44251	42.033818	0.	-1.3518076
66	-12.052774	66.046113	0.	-0.68685718E-01

1 ANSYS - ENGINEERING ANALYSIS SYSTEM REVISION 4.4 A 24 NEW JER
ANSYS(R) COPYRIGHT(C) 1971, 1978, 1982, 1983, 1985, 1987, 1989, 1990 SWAN
PROPRIETARY DATA - UNAUTHORIZED USE, DISTRIBUTION OR DUPLICATION IS PROHIBIT
FOR SUPPORT CALL DAVID PEREL PHONE (201) 596-3356 TWX

Beam Diaphragm structure,clearance=22u
UNIVERSITY VERSION FOR EDUCATIONAL PURPOSES ONLY

***** POST1 ELEMENT NODAL STRESS LISTING *****

LOAD STEP 1 ITERATION= 1 SECTION= 1
TIME= 0. LOAD CASE= 1

THE FOLLOWING X,Y,Z STRESSES ARE IN GLOBAL COORDINATES

NODE	SX	SY	SZ	SXY	SYZ
ELEMENT= 17		STIF 82			
78	78.965001	-38.419705	0.	-88.278662	
80	725.89701	175.01035	0.	-276.73901	
82	-771.15555	-194.65859	0.	282.15668	
76	-100.95525	-64.337404	0.	89.795787	
79	402.43100	68.295325	0.	-182.50884	
81	-22.629274	-9.8241154	0.	2.7088366	
83	-436.05540	-129.49799	0.	185.97624	
77	-10.995124	-51.378554	0.	0.75856206	
ELEMENT= 19		STIF 82			
80	83.803960	1.5334375	0.	30.458438	
92	-71.088461	-27.754791	0.	-25.090339	
90	117.57664	13.231866	0.	-54.378508	
82	-371.83522	-45.433796	0.	145.37664	
93	6.3577493	-13.110677	0.	2.6840497	
91	23.244089	-7.2614626	0.	-39.734424	
89	-127.12929	-16.100965	0.	45.499067	
81	-144.01563	-21.950179	0.	87.917540	
ELEMENT= 20		STIF 82			
92	-76.803300	-19.820388	0.	42.571740	
80	80.455505	17.355785	0.	-54.977931	
95	27.609265	6.7035378	0.	-2.8476324	
95	27.609265	6.7035378	0.	-2.8476324	
93	1.8261025	-1.2323015	0.	-6.2030956	
94	54.032385	12.029661	0.	-28.912782	
95	27.609265	6.7035378	0.	-2.8476324	
96	-24.597017	-6.5584250	0.	19.862054	
ELEMENT= 21		STIF 82			
95	2.1766577	-3.3439661	0.	-7.9235560	
97	7.6744927	-4.7148217	0.	4.1635867	
101	-4.1773771	-10.473564	0.	-4.8284965	
92	8.0975435	3.2321436	0.	10.908174	
134	4.9255752	-4.0293939	0.	-1.8799847	
99	1.7485578	-7.5941931	0.	-0.33245493	
100	1.9600832	-3.6207104	0.	3.0398386	
96	5.1371006	-0.55911288E-01	0.	1.4923088	
ELEMENT= 22		STIF 82			
109	-17.725160	13.135075	0.	9.2096303	

101	-14.855640	-11.259322	0.	-2.0039781
97	26.377865	3.3139117	0.	5.0205807
97	26.377865	3.3139117	0.	5.0205807
108	-16.290400	0.93787653	0.	3.6028261
99	5.7611125	-3.9727050	0.	1.5083013
97	26.377865	3.3139117	0.	5.0205807
98	4.3263526	8.2244932	0.	7.1151055

1 ANSYS - ENGINEERING ANALYSIS SYSTEM REVISION 4.4 A 24 NEW JER
ANSYS(R) COPYRIGHT(C) 1971, 1978, 1982, 1983, 1985, 1987, 1989, 1990 SWAN
PROPRIETARY DATA - UNAUTHORIZED USE, DISTRIBUTION OR DUPLICATION IS PROHIBIT
FOR SUPPORT CALL DAVID PEREL PHONE (201) 596-3356 TWX

Beam Diaphragm structure,clearance=22u
UNIVERSITY VERSION FOR EDUCATIONAL PURPOSES ONLY

***** POST1 ELEMENT NODAL STRESS LISTING *****

LOAD STEP 1 ITERATION= 1 SECTION= 1
TIME= 0. LOAD CASE= 1

THE FOLLOWING X,Y,Z STRESSES ARE IN GLOBAL COORDINATES

NODE	SX	SY	SZ	SXY	SYZ
ELEMENT= 23		STIF 82			
101	-13.723478	-12.310355	0.	-7.1912167	
109	-13.020994	23.990721	0.	25.260643	
110	16.344337	-14.644938	0.	1.4407940	
103	-61.304308	2.1243566	0.	-3.2602439	
108	-13.372236	5.8401831	0.	9.0347132	
107	1.6616717	4.6728915	0.	13.350719	
105	-22.479985	-6.2602906	0.	-0.90972497	
102	-37.513893	-5.0929991	0.	-5.2257303	
ELEMENT= 24		STIF 82			
92	-20.237279	44.103873	0.	47.427964	
101	-50.924737	-30.976961	0.	0.53787925	
103	-22.767856	6.1790636	0.	31.501291	
90	-99.539497	4.7003337	0.	-46.705581	
100	-35.581008	6.5634559	0.	23.982922	
102	-36.846297	-12.398949	0.	16.019585	
104	-61.153677	5.4396987	0.	-7.6021453	
91	-59.888388	24.402103	0.	0.36119134	
ELEMENT= 25		STIF 82			
109	-172.28073	-19.660342	0.	43.160254	
114	-636.13145	6.6663084	0.	-66.223178	
133	586.21924	12.759738	0.	118.70096	
110	122.36852	21.289177	0.	0.99752865	
113	-404.20609	-6.4970167	0.	-11.531462	
112	-24.956104	9.7130232	0.	26.238891	
111	354.29388	17.024458	0.	59.849245	
107	-24.956104	0.81441762	0.	22.078891	
ELEMENT= 26		STIF 82			
114	-532.75290	18.254706	0.	-68.984472	
132	-133.82137	-81.644108	0.	34.051819	
117	111.83112	3.4971142	0.	-11.521581	
133	487.49436	25.726649	0.	116.47100	
106	-333.28714	-31.694701	0.	-17.466326	
115	-10.995124	-39.073497	0.	11.265119	
116	299.66274	14.611882	0.	52.474708	
112	-22.629274	21.990678	0.	23.743263	
ELEMENT= 27		STIF 82			
132	-43.498737	-21.993270	0.	-27.019679	

121	9.9718140	11.497723	0.	-0.38457872
119	3.6500003	-0.30067075E-01	0.	-11.159168
117	88.304588	0.80704706	0.	12.017074
122	-16.763461	-5.2477735	0.	-13.702129
120	6.8109072	5.7338280	0.	-5.7718733
118	45.977294	0.38848999	0.	0.42895295
115	22.402926	-10.593112	0.	-7.5013025

1 ANSYS - ENGINEERING ANALYSIS SYSTEM REVISION 4.4 A 24 NEW JER
ANSYS(R) COPYRIGHT(C) 1971, 1978, 1982, 1983, 1985, 1987, 1989, 1990 SWAN
PROPRIETARY DATA - UNAUTHORIZED USE, DISTRIBUTION OR DUPLICATION IS PROHIBIT
FOR SUPPORT CALL DAVID PEREL PHONE (201) 596-3356 TWX

Beam Diaphragm structure,clearance=22u
UNIVERSITY VERSION FOR EDUCATIONAL PURPOSES ONLY

***** POST1 ELEMENT NODAL STRESS LISTING *****

LOAD STEP 1 ITERATION= 1 SECTION= 1
TIME= 0. LOAD CASE= 1

THE FOLLOWING X,Y,Z STRESSES ARE IN GLOBAL COORDINATES

NODE	SX	SY	SZ	SXY	SYZ
ELEMENT=	28	STIF 82			
121	11.460520	22.468263	0.	-25.837557	(
132	-46.723645	-26.734777	0.	29.689533	(
124	-3.8377556	-49.905716	0.	26.840947	(
124	-3.8377556	-49.905716	0.	26.840947	(
122	-17.631562	-2.1332568	0.	1.9259879	(
123	-25.280700	-38.320246	0.	28.265240	(
124	-3.8377556	-49.905716	0.	26.840947	(
125	3.8113823	-13.718726	0.	0.50169509	(
ELEMENT=	29	STIF 82			
127	-7.7839624	-0.31071833	0.	-1.4652367	(
121	7.4309686	20.919711	0.	-8.4437039	(
124	-18.658693	-54.691683	0.	0.75190194	(
135	17.062333	64.378401	0.	-0.79978445	(
126	-0.17649686	10.304497	0.	-4.9544703	(
125	-5.6138620	-16.885986	0.	-3.8459010	(
136	-0.79818002	4.8433592	0.	-0.23941253E-01	(
131	4.6391851	32.033841	0.	-1.1325106	(
ELEMENT=	30	STIF 82			
121	1.7780098	-3.4012333	0.	-9.3729561	(
127	-4.1796586	6.2258791	0.	-1.8240541	(
129	1.6279301	2.3651269	0.	-2.3543494	(
119	8.5427699	-11.003051	0.	1.9427821	(
126	-1.2008244	1.4123229	0.	-5.5985051	(
128	-1.2758643	4.2955030	0.	-2.0892018	(
130	5.0853500	-4.3189622	0.	-0.20578367	(
120	5.1603899	-7.2021422	0.	-3.7150870	(

PRODUCE DISPLACEMENT PLOT, KUND= 1

PRODUCE STRESS PLOT, LABEL= SX KAVG= 0

***** ROUTINE COMPLETED ***** CP = 16.260

***** END OF INPUT ENCOUNTERED ON FILE18

PREP7 AFWRITE OR SFWRITE WARNING MESSAGES = 1
NUMBER OF SOLUTION PHASE WARNING MESSAGES = 0

Bibliography

[1] J. J. Wortman and L. K. Monteith, Semiconductor Mechanical sensor, IEEE Trans. of Electron Devices, ED-16(1969) 885.

[2] W. H. Ko, J. Hynecek and S. F. Boettcher, Development of a miniature pressure transducers for biomedical applications, IEEE Trans. Electron Devices, ED-26(1979)1887-1896.

[3] W. H. Ko, Solid State Capacitive Pressure Transducers, Sensors and Actuators, 10(1986)303-320.

[4] S. K. Clark and K. D. Wise, Pressure Sensitivity in an Anisotropically etched Thin Diaphragm Pressure Sensors, IEEE Trans. Electron Devices, ED-26(1979)1887-1896.

[5] O. N. Tufte, P. W. Chapman, and D. Long, Silicon Diffused Element Piezoresistive Diaphragm, J. Appl. Phy. , 33(1962) 3322-3327.

[6] S. Timoshenko, Theory of Plates and Shells, Mcgraw hill, New York, 1940.

[7] H. L. Chan and K. D. Wise, Scaling Limits in Batch Fabricated Silicon Pressure Sensors, Tech. Digest, Transducers'85, Philadelphia, June 11-14, 1985, pp174-177.

[8] M. Shimazoe, Y. Matsuka, A. Yasukawa and M. Tanabe, A special Silicon Diaphragm Pressure Sensor with High Output and High Accuracy, Sensors and Actuators, 2(1982)275-282.

[9] R. M. Whitter, Basic advantages of Anisotropic Etched, Transverse Gauge Pressure Transducers, Endevco Tech. Paper, TP 277.

[10] J. Mallon, F. Pourahmadi, K. Peterson, P. Barth, T. Vermeulen and J. Bryzek, Low Pressure Sensors Employing Bossed Diaphragm and Precision Etch Stopping, Sensors and Actuators, 1990.

[11] Ming Hang Bao, L. Z. Yu and Y. Wang, Micromachined Beam diaphragm Structure Improves Performance of Pressure Transducers, Sensors and Actuators, 1990.

[12] L. B. Wilner, A Diffused Silicon Pressure Transducer with Stress Concentration at Transverse Gauges, 23rd Int. Instrumentation Symp., Las Vegas, NV, May1977.

[13] J. W. Beams, Mechnical Properties of Thin Film of Gold and Silver, in Structure and Properties of Thin Films, ed. C. A. Neugebauer, J. B. Newkirk, and D. A. Vermilyea, John Wiley Sons, New York, pp 183-192, 1959.

[14] Pinyen Lin, The in-situ measurement of mechanical properties of multilayer coatings, Ph. D. Thesis, Massachusetts Institute of Technology, June 1990.

[15] A. Yasukawa, S. Shimada, Y. Matusuoka, and Y. Kanda, Design Consideration for Silicon Circular Diaphragm Pressure Sensor, Japanese J. of Appl. Phys., 21(7), 1049, 1982.

[16] M. G. Allen, M. S. Thesis, Department of Chemical Engineering, Massachusetts Institute of Technology, Cambridge, Mass. 1986.

[17] O. C. Zienkiewicz, The Finite Element Method, Chap.2, McGraw Hill, New York, 1977.

[18] K. Petersen, Silicon as a Mechanical Material, Proceedings of IEEE, Vol. 70, No.5, May 1982.

[19] W. G. Pfann and R. N. Thurston, Semiconducting Stress Transducers utilizing the transverse and shear Piezoresistive Effects, J. of Appl. Phys., vol. 32-10, Oct. 1961.

[20] O. N. Tufte, and E. L. Stelzer, Piezoresistive Properties of Silicon Diffused Layers, J. of Appl. Phys. , Vol. 34, pp 313-318, Feb. 1963.

[21] S. M. Sze, Semiconductor Devices, 1985.

[22] H. C. Nathanson, Resonant Gate Transistor, IEEE Tran. Electron Devices, pp 117-133, 1967.

[23] T. L. Poteat, Submicron Accuracies in Anisotropically Etched Silicon Piece Parts-A Case Study, Micromachining and Micropackaging of Transducers, Elsvier Publishers, pp 151-158, 1985.

[24] Y. Kanda, A Graphical Representation of the Piezoresistance Coefficients in Silicon, IEEE Trans. on Electron Devices, ED-29, No. 1, pp 64-70, Jan. 1982.

[25] A. Bong, Ethelene diamine-pyrocatechol-water mixture shows etching anomaly in boron doped silicon, J. Electrochem. Soc., 118(1971)401-402.